Journal of Medicinal Chemistry

Article

pubs.acs.org/jmc

Synthesis and Biological Evaluation of Novel σ_1 Receptor Ligands for Treating Neuropathic Pain: 6-Hydroxypyridazinones

Xudong Cao,[†,§] Yin Chen,[‡,§] Yifang Zhang,[†] Yu Lan,[†] Juecheng Zhang,[†] Xiangqing Xu,[‡] Yinli Qiu,[‡] Song Zhao,[‡] Xin Liu,[†] Bi-Feng Liu,[†] and Guisen Zhang*[,†,‡]

[†]Systems Biology Theme, Department of Biomedical Engineering, College of Life Science and Technology, Huazhong University of Science and Technology, Wuhan 430074, China

[‡]Jiangsu Nhwa Pharmaceutical Co., Ltd., 69 Democratic South Road, Xuzhou, Jiangsu 221116, China

Supporting Information

ABSTRACT: By use of the 6-hydroxypyridazinone framework, a new series of potent σ_1 receptor ligands associated with pharmacological antineuropathic pain activity was synthesized and is described in this article. In vitro receptor binding studies revealed high σ_1 receptor affinity (K_i σ_1 = 1.4 nM) and excellent selectivity over not only σ_2 receptor (1366-fold) but also other CNS targets (adrenergic, μ-opioid, sertonerigic receptors, etc.) for 2-(3,4-dichlorophenyl)-6-(3-(piperidin-1-yl)propoxy)pyridazin-3(2*H*)-one (compound **54**). Compound **54** exhibited dose-dependent antiallodynic properties in mouse formalin model and rats chronic constriction injury (CCI) model of neuropathic pain. In addition, functional activity of compound **54** was evaluated using phenytoin and indicated that the compound was a σ_1 receptor antagonist. Moreover, no motor impairments were found in rotarod tests at antiallodynic doses and no sedative side effect was evident in locomotor activity tests. Last but not least, good safety and favorable pharmacokinetic properties were also noted. These profiles suggest that compound **54** may be a member of a novel class of candidate drugs for treatment of neuropathic pain.

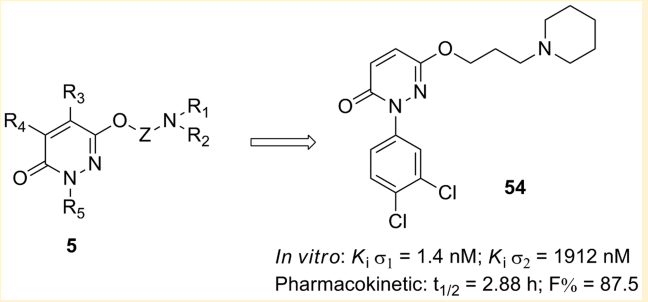

INTRODUCTION

Neuropathic pain is serious and chronic and thus greatly impacts quality of life, which can be relieved but cannot be cured.[1] Its exact incidence and prevalence are unknown, but overall prevalence is conservatively estimated at 3−8% of the general population in developed countries.[2,3] Unfortunately, all currently available treatments afford only modest alleviation of pain and minimal improvements in physical and emotional functioning.[4] Although very intensive research efforts have improved our understanding of the mechanisms that cause pain, those efforts have not yet yielded new antineuropathic pain drugs.[5] In the absence of any real breakthrough in antiallodynic drugs development, current guidelines for the management of neuropathic pain feature only incremental improvements in existing therapies, including combination treatments, new formulations of existing drugs, me-too drugs, and refinements based on supposed drug mechanisms of action.[6−9] Among these, tricyclic antidepressants, dual serotonin−norepinephrine reuptake inhibitors (duloxetine), calcium channel α_2-δ ligands (gabapentin and prebagalin), and topical lidocaine are recommended as first-line therapy for neuropathic pain.[7−9] Opioid antiallodynic drugs are typically recommended for patients who have not responded to first-line medications.[10,11] Although these medications are effective in reducing pain in neuropathic pain disorders, they may cause serious side effects such as weight gain and hyperalgesia and carry significant risk of addiction.[10,11] Thus, the new antineuropathic pain agents with novel mechanisms of action that improved the efficacy of existing therapies and reduced the adverse effects are wanted.

Pharmacological studies and biochemical analyses have shown that σ receptors represent a unique, non-opioid, non-phencyclidine, haloperidol-sensitive receptor family.[12,13] Two distinct subtypes, termed the σ_1 and σ_2 receptors, have been characterized. The σ_1 receptor has been cloned from several species and various tissues; the protein is 223 amino acids long and has a molecular weight of 25.3 kDa.[14,15] Functionally, σ_1 receptor interacts physically with several receptors and ion channels, or elements of their transduction machineries, to modulate receptor/ion channel activities.[16] The receptor behaves as a unique ligand-regulated molecular chaperone modulating the activities of various proteins and ion channels, including the K^+ and Ca^{2+} channels, and the *N*-methyl-D-aspartate (NMDAR) and opioid receptors, all of which are involved in pain.[17−21] σ_1 receptor is expressed in regions important in terms of pain control; these include dorsal root ganglion neurons, the dorsal spinal cord, the periaqueductal gray matter, and the rostroventral medulla.[16] Receptor expression in the spinal cord is upregulated during the

Received: September 12, 2015

DOI: 10.1021/acs.jmedchem.5b01416
J. Med. Chem. XXXX, XXX, XXX−XXX

induction phase of neuropathic pain.[22,23] The pharmacological profiles of σ_1 receptor and σ_2 receptor differ, and both proteins may serve as biomarkers of tumor cell proliferation and proapoptotic tendencies.[24] The proteins may thus play roles in cancer imaging and treatment.[25,26]

To date, mounting evidence indicates that targeting σ receptors may be particularly beneficial in a number of neurodegenerative conditions including Alzheimer's disease, Parkinson's disease, stroke, methamphetamine neurotoxicity, Huntington's disease, amyotrophic lateral sclerosis, and retinal degeneration.[27] The putative σ_1 receptor antagonist, SN79 (6-acetyl-3-(4-(4-(4-fluorophenyl)piperazin-1-yl)butyl)benzo[*d*]-oxazol-2(3*H*)-one), can attenuate psychostimulant effects.[28] The selective σ receptor ligand, AC927 (1-(2-phenethyl)-piperidine oxalate), can block several cocaine effects that are related to its abuse and excessive intake.[29] Various 2(3*H*)-benzoxazolones and 2(3*H*)-benzothiazolones have been reported as highly selective σ_1 receptor ligands, and ^{18}F-labeled 2(3*H*)-benzothiazolones were developed as potential positron emission tomography (PET) candidate radioligands for imaging σ receptors in the central nervous system (CNS).[30] In addition, many selective σ_1 receptor ligands have been tested as treatments for CNS disorders in clinical studies.[31−35] Moreover, based on the recent preclinical data, selective σ_1 receptor antagonists may be both efficacious and safe when used to counter difficult-to-treat chronic pain (including neuropathic pain) and to enhance (or maintain) antiallodynic efficacy and increase the safety margins of opioid doses.[36] BD-1063 (**1**) is a typical σ_1 receptor antagonist, inhibiting mechanical allodynia induced by capsaicin.[37,38] The recently described σ_1 receptor antagonists, S1RA (**2**), have good safety, tolerability, and pharmacokinetic profiles and are currently in phase II clinical trials for treatment of neuropathic pain.[39,40] Recently, a series of 4-aminotriazoles (**3**) exhibiting nanomolar potency for σ_1 receptor and good selectivity (compared to σ_2 receptor) has been reported[41] (Figure 1).

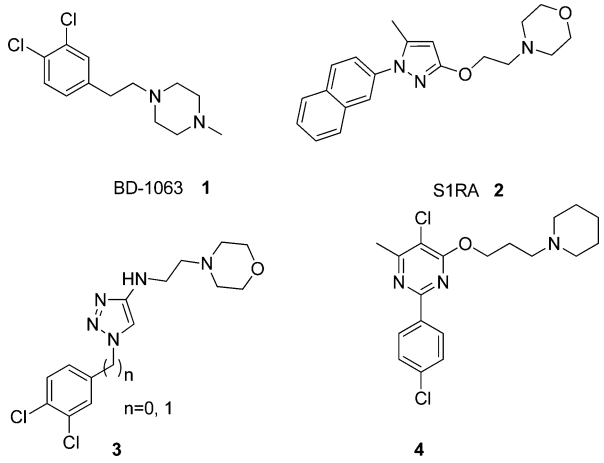

Figure 1. Representative σ_1 receptor ligands.

Our interest has focused on the development of novel ligands with high affinity to the σ_1 receptor and selectivity over the σ_2 receptor subtype.[42,43] Recently, the pharmacophoric model of Glennon et al.,[44,45] (Figure 2A) was used to build a 3D pharmacophore model allowing virtual drug screening. Hit analysis showed that a pyrimidine scaffold was important, and we prepared a series of such compounds. Compound **4**

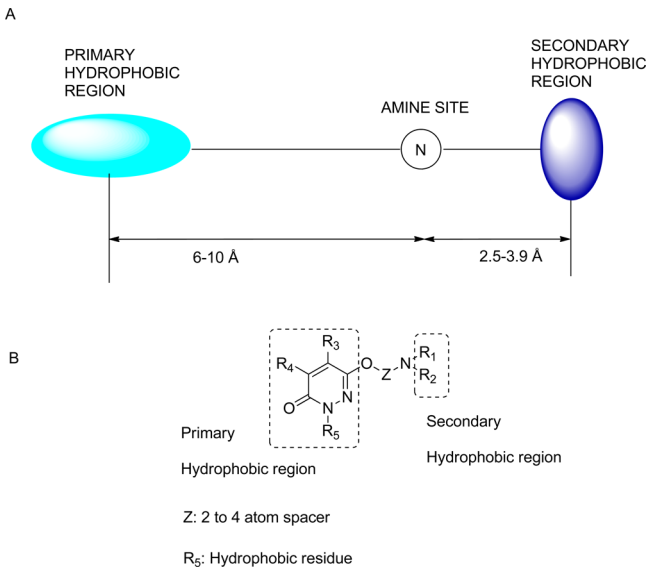

Figure 2. Glennon's pharmacophoric σ_1 receptor model (A) and general structure of the new pyridazinone derivative (B).

exhibited a good pharmacophoric profile, binding to σ_1 receptor, implicated in pain.[43]

Pyridazine and pyrimidine are isomeric compounds in which two nitrogen atoms differ in position. Pyridazine and its oxygenated derivative pyridazinone contain well-studied six-membered heterocyclic rings. These compounds exhibit various pharmacological activities and are present in many natural sources.[46,47] The compounds based on pyridazine or pyridazinone scaffold have recently been shown to increase CNS activity. Specifically, selective histamine H_3 receptor ligands contained the pyridazinones were reported as lead candidates for potential use in the treatment of chronic pain and cognitive disorders.[47]A novel series of phosphodiesterase 10A inhibitors based on pyridazine or pyridazinone rings were reported as clinical candidate for the treatment of schizophrenia.[48] To further explore novel σ_1 ligands, we focused on ring bioisosteres of the pyrimidine moiety.[49] We introduced the pyridazinone ring 6-hydroxy-2-phenylpyridazinone, combined with the basic amino moiety, by molecular hybridization[50] to form a new series of ligands (**5**) with high affinity to the σ_1 receptor and selectivity over the σ_2 receptor subtype (Figure 3).

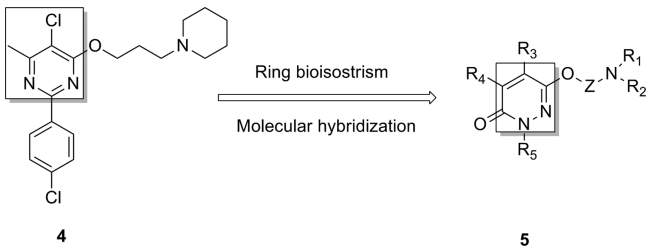

Figure 3. Design of new pyridazinone derivatives.

This strategy yielded a series of new compounds (Tables 1−5), which were used in SAR (structure−activity relationship) studies to evaluate their pharmacological efficacy and in competitive receptor-binding assays to determine relative affinity for σ_1 and σ_2 receptors. Among the derivatives prepared, compound **54** exhibited high affinity for the σ_1 receptor and low affinity for the σ_2 receptor. Further, compound **54** exerted

DOI: 10.1021/acs.jmedchem.5b01416
J. Med. Chem. XXXX, XXX, XXX−XXX

Table 1. Binding Affinities for the σ_1 and σ_2 Receptor of Compounds 12−23

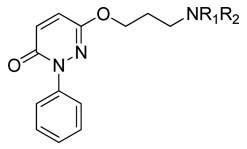

12-23

Compd	NR_1R_2	$K_i\sigma_1$(nM)[a]	$K_i\sigma_2$(nM)[b]	Selectivity (σ_2/σ_1)
12	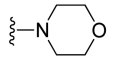	66.3±6.0[c]	502±49.2	7.6
13	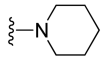	21.4±2.5	1074±96	50.2
14	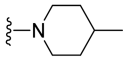	28.0±3.4	1464±101	52.3
15	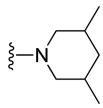	46.0±4.1	1822±148	39.6
16	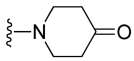	580±41.9	>2000	----
17	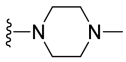	31.7±3.5	376±34	11.9
18	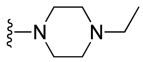	40.1±3.5	620±67	15.5
19	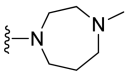	30.3±2.8	508±54	16.8
20		35.5±3.8	458±54	12.9
21		108±9.8	818±87	7.57
22	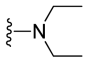	96.5±8.5	1170±121	12.1
23	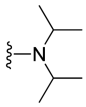	98.1±7.9	1120±101	11.4
2		10.5 ±0.7	>2000	----

[a]Affinities were determined in guinea pig brain using [^{3}H]-(+)-pentazocine. [b]Affinities were determined in guinea pig brain using [^{3}H]-DTG in the presence of (+)-SKF-10047 to block σ_1 receptors. [c]The values are the mean ± SEM of three experiments performed in duplicate.

dose-dependent antiallodynic effects in the mouse formalin-induced pain model and the rats CCI model. In addition, function activity of compound **54** was evaluated using phenytoin and indicated that the compound was a σ_1 receptor antagonist. Moreover, no motor impairments were found in rotarod tests at antiallodynic doses and no sedative side effects were evident in locomotor activity tests, and the pharmacokinetic properties were favorable. Thus, compound **54** is a novel compound with great potential for the treatment of neuropathic pain.

CHEMISTRY

Compounds were synthesized according to the reaction pathways illustrated in Schemes 1−3. As depicted in Scheme 1, phenylaminoalkoxypyridazinone derivatives were prepared using two alternative procedures. The key intermediate 6-hydroxy-2-phenylpyridazin-3(2*H*)-one **8** was obtained via one-step cyclization with phenylhydrazine hydrochloride **6** and maleic anhydride **7**. According to the substitution pattern, the final compounds **9** and **12−26** were prepared using method A or the two-step procedure, method B (Tables 1 and 2). In method A, **8** was reacted with commercially available 1-(2-chloroethyl)piperidine under basic conditions to obtain compound **9** in high yield. In method B, the intermediates **10** and **11** were produced by the alkylation with **8** and **1**, *n*-dibromoalkanes, and then reacted with the corresponding amines under mild basic conditions to afford the final compounds **12−26**.

The route depicted in Scheme 2 was used to prepare substituted pyridazinone scaffold compounds **50−60** and **62−**

DOI: 10.1021/acs.jmedchem.5b01416
J. Med. Chem. XXXX, XXX, XXX−XXX

Scheme 1[a]

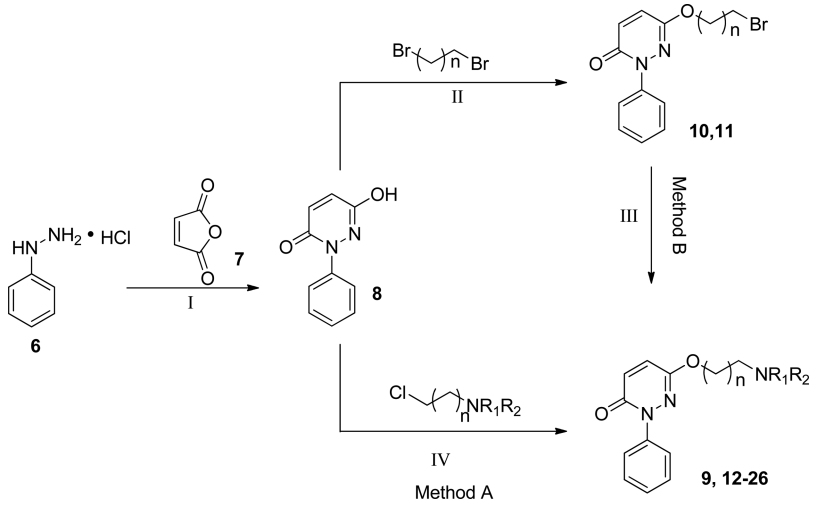

[a]Reagents and conditions: (I) H_2O, conc HCl, reflux; (II) $Br(CH_2)_{n+1}Br$, K_2CO_3, acetone, reflux; (III) HNRR, K_2CO_3, KI, acetonitrile, reflux; (IV) K_2CO_3, KI, acetonitrile, reflux.

Table 2. Binding Affinities for the σ_1 and σ_2 Receptor of Compounds 9, 13, 14, and 24−26

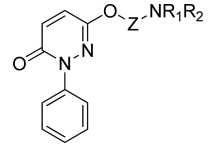

9, 24-26

Compd	Z	NR_1R_2	$K_i\sigma_1$(nM)[a]	$K_i\sigma_2$(nM)[b]	Selectivity (σ_2/σ_1)
13	$(CH_2)_3$	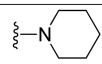	21.4±2.5[c]	1074±96	50.2
14	$(CH_2)_3$	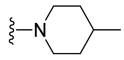	28.0±3.4	1464±101	52.3
9	$(CH_2)_2$	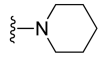	>2000	>2000	----
24	$(CH_2)_4$	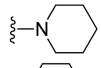	124±13	1722±169	13.9
25	$(CH_2)_4$	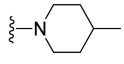	143±13	1440±120	10.1
26	$(CH_2)_4$	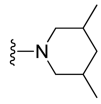	222±23	1370±152	6.2

[a]Affinities were determined in guinea pig brain using [^{3}H]-(+)-pentazocine. [b]Affinities were determined in guinea pig brain using [^{3}H]-DTG in the presence of (+)-SKF-10047 to block σ_1 receptors. [c]The values are the mean ± SEM of three experiments performed in duplicate.

72. The intermediates **27−38** were obtained using the cyclization procedure with substituted phenylhydrazine hydrochloride, which was reacted with maleic anhydride **7**, depending on the substitution pattern of the final pyridazinone. Next, standard alkylation with 1,3-dibromopropane was conducted to produce **39−49**, and then reaction with the piperidine or 4-methylpiperidine afforded the final compounds **50−60** and **62−72**, respectively, in moderate yields (Tables 3 and 4). Compound **61** was obtained by reaction with commercially available 1-(3-chloropropyl)piperidine, and intermediate **38**, under basic conditions (Table 3).

The route depicted in Scheme 3 was used to prepare the substituted pyridazinone scaffold compounds **79−81**. Intermediates **73−75** were obtained by cyclization of 3,4-dichlorophenylhydrazine hydrochloride with various substituted maleic anhydrides, depending on the substitution patterns desired in the final pyridazinones. Next, standard alkylation with 1,3-dibromopropane produced compounds **76−78**, and reaction with piperidine afforded the final compounds **79−81**, respectively, in moderate yields (Table 5).

Indeed, the 1-phenyl-1,2-dihydropyridazine-3,6-dione and 6-hydroxy-2-phenylpyridazin-3(2*H*)one are ambident tautomeric

DOI: 10.1021/acs.jmedchem.5b01416
J. Med. Chem. XXXX, XXX, XXX−XXX

Scheme 2[a]

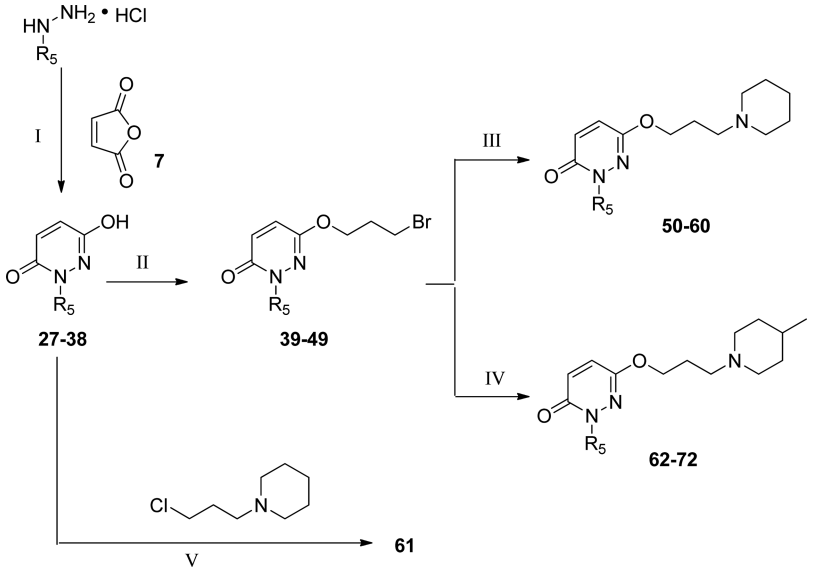

[a]Reagents and conditions: (I) H_2O, conc HCl, reflux; (II) $Br(CH_2)_3Br$, K_2CO_3, acetone, reflux; (III) piperidine, K_2CO_3, KI, acetonitrile, reflux; (IV) 4-methylpiperidine, K_2CO_3, KI, acetonitrile, reflux; (V) K_2CO_3, KI, acetonitrile, reflux.

Table 3. Binding Affinities for the σ_1 and σ_2 Receptor of Compounds 13 and 50−61

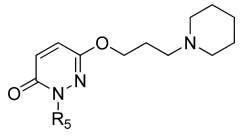

50-61

compd	R_5	K_i σ_1 (nM)[a]	K_i σ_2 (nM)[b]	selectivity (σ_2/σ_1)
13	phenyl	21.4 ± 2.5[c]	1074 ± 96	50.2
50	4-methylphenyl	69.0 ± 7.2	1280 ± 120	18.6
51	2-naphthyl	74.1 ± 8.9	895 ± 95	12.1
52	4-fluorophenyl	17.0 ± 2.0	>2000	–
53	4-chlorophenyl	9.8 ± 1.4	1573 ± 127	160.5
54	3,4-dichlorophenyl	1.4 ± 0.1	1912 ± 210	1365.7
55	2,3-dichlorophenyl	48 ± 2.1	1617 ± 184	33.6
56	3,5-dichlorophenyl	30 ± 1.2	1301 ± 89	43.3
57	2,4-dichlorophenyl	25 ± 2.1	809 ± 15	32.3
58	2,5-dichlorophenyl	45 ± 2.3	902 ± 10	20.0
59	3-chloro-4-fluorophenyl	10 ± 1.3	1581 ± 120	158.1
60	3,4-difluorophenyl	8 ± 1.9	1908 ± 130	238.5
61	cyclopentyl	>2000	>2000	–

[a]Affinities were determined in guinea pig brain using [^{3}H]-(+)-pentazocine. [b]Affinities were determined in guinea pig brain using [^{3}H]-DTG in the presence of (+)-SKF-10047 to block σ_1 receptors. [c]The values are the mean ± SEM of three experiments performed in duplicate.

heterocyclic. They are produced via a cyclization of the phenylhydrazine hydrochloride **6** and maleic anhydride **7** in the presence of acetic acid as solvent.[51] In this paper, 6-hydroxy-2-phenylpyridazin-3(2*H*)-one (**8**) was prepared in solution of water and hydrochloric acid. When the tautomeric pyridazinones were reacted with compound **1**, *n*-dibromoalkane, chemoselectivity may be in play. The N-alkylation products were obtained when 1-phenyl-1,2-dihydropyridazine-3,6-dione was reacted with **1**, *n*-dibromoalkane in the presence of acetonitrile with K_2CO_3.[52,53] While acetonitrile was replaced with acetone, 6-hydroxy-2-phenylpyridazin-3(2*H*)one was treated with **1**, *n*-dibromoalkane, and the O-alkylation product may be obtained mainly. To determine the absolute configuration, the most active compound **54** (Table 3) was subjected to single crystal X-ray diffraction (SCXRD). As no suitable crystals were obtained using the free base, limited salt screening was performed. The hydrochloride yielded crystals suitable for SCXRD, by which a relative configuration was reliably determined. As shown in Figure 4, this confirmed the selectivity assigned above. The result indicates indirectly that 6-hydroxy-2-phenylpyridazin-3(2*H*)-one was prepared in solution of water and hydrochloric acid and the O-alkylation product was obtained mainly during the alkylation.

RESULTS AND DISCUSSION

Structure−Activity Relationships. The new series of pyridazinone derivatives was designed to exploit the known pharmacophoric features of σ_1 receptor ligands. As recently

DOI: 10.1021/acs.jmedchem.5b01416
J. Med. Chem. XXXX, XXX, XXX−XXX

Table 4. Binding Affinities for the σ_1 and σ_2 Receptor of Compounds 14 and 62−72

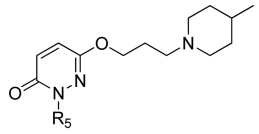

62-72

compd	R_5	K_i σ_1 (nM)[a]	K_i σ_2 (nM)[b]	selectivity (σ_2/σ_1)
14	phenyl	28.0 ± 3.4[c]	1464 ± 101	52.3
62	4-methylphenyl	61.6 ± 65	1549 ± 135	25.1
63	2-naphthyl	84.1 ± 9.1	913 ± 10.4	10.8
64	4-fluorophenyl	19.8 ± 2.4	1619 ± 147	81.7
65	4-chlorophenyl	9.5 ± 1.2	1783 ± 210	187.7
66	3,4-dichlorophenyl	5.0 ± 0.6	1742 ± 198	348.4
67	2,3-dichlorophenyl	55 ± 2.3	1201 ± 34	21.8
68	3,5-dichlorophenyl	43 ± 1.4	1321 ± 57	30.7
69	2,4-dichlorophenyl	35 ± 2.6	1100 ± 23	31.4
70	2,5-dichlorophenyl	60 ± 3.4	870 ± 15	14.5
71	3-chloro-4-fluorophenyl	10 ± 1.4	1627 ± 36	162.7
72	3,4-difluorophenyl	15 ± 1.2	1701 ± 45	113.4

[a]Affinities were determined in guinea pig brain using [^{3}H]-(+)-pentazocine. [b]Affinities were determined in guinea pig brain using [^{3}H]-DTG in the presence of (+)-SKF-10047 to block σ_1 receptors. [c]The values are the mean ± SEM of three experiments performed in duplicate.

Scheme 3[a]

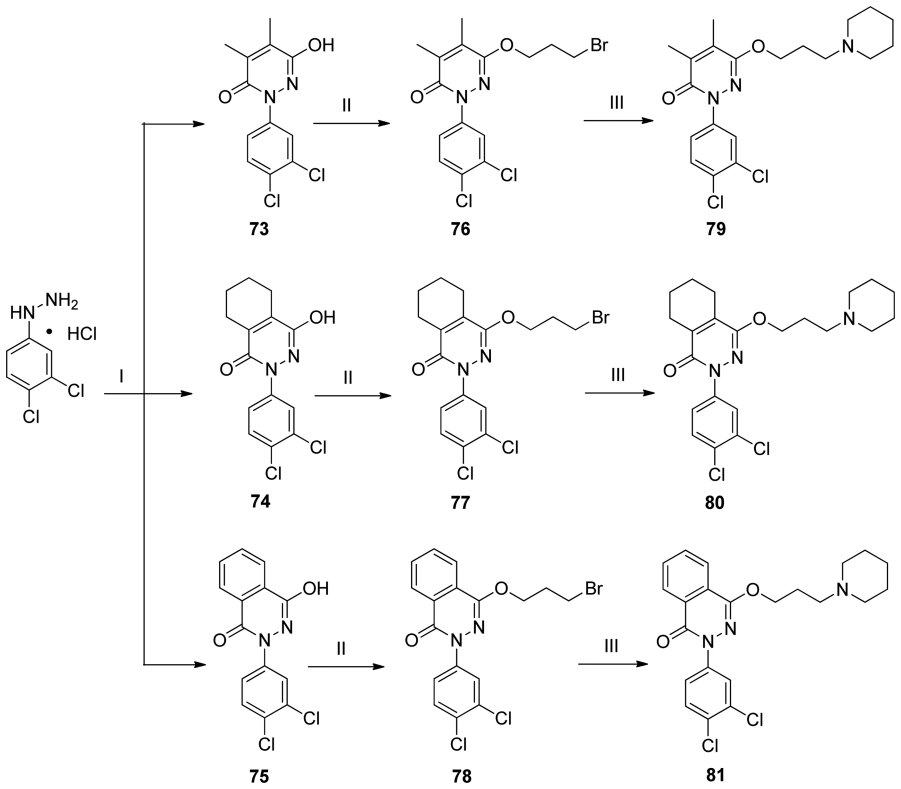

[a]Reagents and conditions: (I) H_2O, conc HCl, reflux; (II) $Br(CH_2)_3Br$, K_2CO_3, acetone, reflux; (III) piperidine, K_2CO_3, KI, acetonitrile, reflux.

summarized by Glennon et al., σ_1 receptor ligands should contain a basic amino group and no fewer than two hydrophobic regions at specified distances from the amino group, thus 2.5−3.9 and 6−10 Å.[44,45](Figure 2A). Compounds of this general structure (Figure 2B) were designed in which the pyridazinones served as scaffolds bearing various groups meeting the pharmacophoric requirements; certain variations were also included. In detail, the chemical structures of these pyridazinone derivatives were designed according to the following rationale: we tested various basic amino moieties to fit the amine site and secondary hydrophobic region (NR1R2), changed the distance between the pyridazinone ring and basic amino moiety (carbon chain linker) to meet the pharmacophoric requirements, replaced the 2-phenyl goup of pyridazinone by an aromatic ring or aliphatic ring (R5), and took different substitution on the 4- and 5-positions of the

DOI: 10.1021/acs.jmedchem.5b01416
J. Med. Chem. XXXX, XXX, XXX−XXX

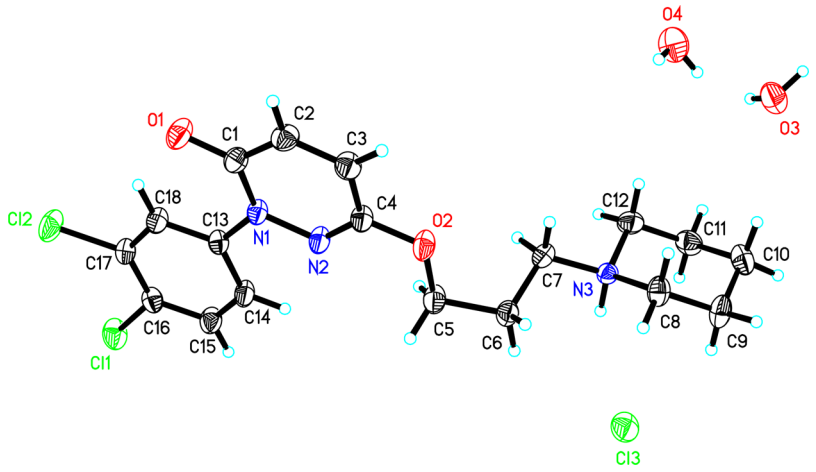

Figure 4. ORTEP showing the molecular structure of the hydrochloride salt of **54**.

pyridazinone ring (R3 and R4) to find the best conformational fitting to the receptor.

The new compounds were first evaluated in vitro by determining their binding affinities for the σ_1 and σ_2 receptors. [^{3}H](+)-Pentazocine was used determining binding at σ_1 receptor. Affinity at σ_2 receptor was determined using [^{3}H]di-*o*-tolylguanidine in the presence of (+)-SKF-10047 (to block the σ_1 receptor), respectively.[36,54] The results of these primary assays are shown in Tables 1−5.

Effect of the Basic Amino Moiety for Different Amine Moieties. In our previous work, the σ_1 receptor ligands (pyrimidines derivatives and 3,4-dihydroxy-2(1*H*)-quinolinone derivatives) designed were consistent with the known pharmacophoric features summarized by Glennon et al. Along with full explorations of SAR, the optimal chain length between the pyrimidine ring (or 3,4-dihydroxy-2(1*H*)-quinolinone scaffold) and the basic amino moiety for high affinity to the σ_1 receptor was determined to be three carbons.[42,43]

In this work, our initial investigation focused on the effect of various basic amino moieties (Table 1, compounds **12**−**23**). First, the morpholine group (**12**) was used because of its frequent appearance in σ_1 receptor ligands, such as **2**, yielding moderate affinity (K_i σ_1 = 66.3 ± 6.0 nM and K_i σ_2 = 502 ± 49.2 nM) to both receptors. Next, the improvements of compounds with regard to hydrophobicity over a morpholino group, piperidine, 4-methylpiperidine, 3,5-dimethylpiperidine (**13**−**15**) were selected, resulting in compound **13**, which showed significantly improved σ_1 receptor binding affinity and selectivity (K_i σ_1 = 21.4 ± 2.5 nM and K_i σ_2 = 1074 ± 96 nM). Increasing the hydrophobicity of piperidinyl by adding a methyl group on the ring (**14**) led to similar binding affinity (K_i σ_1 = 28.0 ± 3.4 nM and K_i σ_2 = 1464 ± 101 nM) to compound **13**, as was observed for compound (**15**), bearing 3,5-dimethylpiperidine (K_i σ_1 = 46.0 ± 4.1 nM and K_i σ_2 = 1822 ± 148 nM). Substituting the oxygen atom of the morpholine with a carbonyl group (**16**) greatly decreased affinity to the σ_1 receptor.

When piperazine was substituted with small alkyl groups (methyl or ethyl), the resulting compounds (**17**, **18**) bound with high affinity to the σ_1 receptor but showed weak selectivity over the σ_2 receptor. The same activity was observed in the larger diazepane or smaller pyrolidine derivative, compound **19** (K_i σ_1 = 30.3 ± 2.8 nM and K_i σ_2 = 508 ± 54 nM), and compound **20** (K_i σ_1 = 35.5 ± 3.8 nM and K_i σ_2 = 458 ± 54 nM). Open-chain amines (**21**−**23**) did not enhance binding affinity or σ_1 receptor selectivity.

It is consistent with the previous work that the nature of the surrounding of the tertiary amine nitrogen had a profound impact on affinity.[30c]

Effect of the Distance between the Pyridazinone Ring and the Basic Amino Moiety. The effect of the length of the linker between the pyridazinone and the basic amino moiety was determined. As shown in Table 2, changes in linker length to two (**9**) or four (**24**−**26**) carbon atoms significantly reduced binding to both the σ_1 and σ_2 receptors. Therefore, the binding affinities for both receptors were dependent upon chain length. Compared to compound **13**, the use of a linker containing two carbon atoms to connect to the piperidine ring (**9**) inactivated binding to both receptors; replacement of the linker with four carbon atoms (**24**) reduced the binding affinity for σ_1. When substituted piperidine rings were used, compounds **25** and **26**, with linkers of four carbon atoms, had low σ_1 receptor and σ_2 receptor affinities. Thus, the alkyl chain length appeared to directly affect the affinities for the two receptors. Together, the data show that a linker of three carbon atoms (compounds **13** and **14**) was optimal. It is consistent with the previous work that three carbons showed high affinity to the σ_1 receptor and excellent selectivity to σ_2 receptor.[42,43]

Effect of Substitution on the 2-Position of the Pyridazinone Ring. Compounds exhibiting good binding affinities and selectivities (**13** and **14**), containing piperidinyl or 4-methylpiperidinyl groups as amino moieties with three-carbon linker, were selected for further SAR investigation. The effects of replacing the phenyl group at the 2-position of the pyridazinone ring with other aromatic or aliphatic rings were explored (Tables 3 and 4).

When the amine moiety was piperidine (Table 3), compound **50** containing electron-donating group (methyl) on the phenyl group retained moderate activity (albeit less than compound **13**) and exhibited lower selectivity. Compound **51** was produced by replacing the phenyl with a naphthyl ring, which did not improve the binding affinity or selectivity. Compounds **52**−**54** contained halogens substituent on the phenyl group, remarkably increasing binding affinity and selectivity; the fluorine-containing compound's (**52**) constants were K_i σ_1 = 17.0 ± 2.0 nM and K_i σ_2 > 2000 nM, while those for the chlorine-bearing molecule (**53**) were K_i σ_1 = 9.8 ± 1.4 nM and K_i σ_2 = 1573 ± 127 nM. Next, the 3,4-dichlorophenyl

DOI: 10.1021/acs.jmedchem.5b01416
J. Med. Chem. XXXX, XXX, XXX−XXX

Table 5. Binding Affinities for the σ_1 and σ_2 Receptor of Compounds 54 and 79−81

Compd	Structure	$K_i\sigma_1$(nM)[a]	$K_i\sigma_2$(nM)[b]	Selectivity (σ_2/σ_1)
54	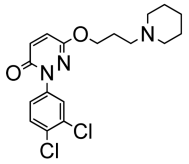	1.4±0.1[c]	1912±210	1365.7
79	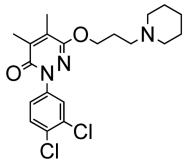	66.6±15	1429±95	21.4
80	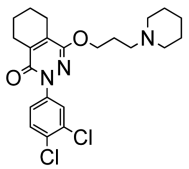	104±9.1	934±12.1	8.9
81	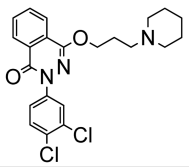	140±2.4	1514±113	10.8

[a]Affinities were determined in guinea pig brain using [^{3}H]-(+)-pentazocine. [b]Affinities were determined in guinea pig brain using [^{3}H]-DTG in the presence of (+)-SKF-10047 to block σ_1 receptors. [c]The values are the mean ± SEM of three experiments performed in duplicate.

group [present in the known σ_1 receptor ligands **1** and **3**] was introduced, and compound **54** had even higher affinity to σ_1 and excellent selectivity over σ_2 (K_i = 1.4 ± 0.1 nM and K_i σ_2 = 1912 ± 210 nM). Substituting other dichlorophenyls for the 3,4-dichlorophenyl group yielded compounds **55**−**58**, which showed lower activity than **54** but with moderate selectivities. Some activity (albeit less than that of compound **54**) was retained upon replacement of the 3,4-dichloro moiety with 3-chloro-4-fluoro or 3,4-difluoro substituents (**59**, **60**); this improved selectivity about 4- to 10-fold compared to compounds **55**−**58**. Replacing the aromatic rings at the 2-position with cyclopentyl **61** resulted in a marked reduction in the affinities for the receptors.

Compounds bearing the amine moiety 4-methylpiperidine (Table 4), **62** with a methyl on the phenyl group and **63** with a naphthyl ring, displayed low affinities for the σ_1 receptor. Again, introduction of halogens on the phenyl group remarkably increased binding affinity and selectivity: for fluorine (**64**), constants were K_i σ_1 = 19.8 ± 2.4 nM and K_i σ_2 = 1619 ± 147 nM, for chlorine (**65**), K_i σ_1 = 9.5 ± 1.2 nM and K_i σ_2 = 1783 ± 210 nM, and for the 3,4-dichloro (**66**), K_i σ_1 = 5.0 ± 0.6 nM and K_i σ_2 = 1742 ± 198 nM. Introduction of other dihalophenyl groups yielded compounds **67**−**72**, which behaved as did the analogs that contained piperidinyl ring (**55**−**60**), confirming the important contribution of the 3,4-dichlorophenyl group to σ receptor affinity.[36,39,41]

Effect of Replacing Groups on the 4- and 5-Positions of the Pyridazinone Ring. The presence of a 3,4-dichlorophenyl group on the 2-position of the pyridazinone ring afforded the best receptor-binding affinity and selectivity, and a three-carbon linker optimally matched the pharmacophoric requirement. Thus, compound **54** was selected for further investigation of the SAR.

We first explored the effects of replacing the hydrogen atom with a methyl group (Table 5, compound **79**). Compound **79** (compared to **54**) for σ_1 and σ_2 receptors had a detrimental effect on affinities, attributable either to the size of the group or to its hydrophobicity. Substitution of the methyl group with a cyclohexyl (**80**) or phenyl (**81**) group significantly decreased receptor affinities even further; large group sizes may have hindered receptor binding.

Overall, compounds **53**, **54**, **59**, **60**, **65**, **66**, **71**, and **72** exhibited affinity for the σ_1 receptor (K_i < 15 nM) with selectivity (compared to σ_2 receptor; >100-fold). Therefore, these compounds were selected for further studies.

Human Ether-a-Go-Go-Related Gene (hERG) Channel Blockade. Recent studies have shown that many medications can prolong the time between the start of the Q wave and the end of the T wave as shown on an electrocardiogram (the QT interval).[55] Indeed, efforts to predict the risk of long-QT syndrome have focused on assays that explore hERG channel activity.[55a] This is because hERG channel blockade is an important indicator of potential proarrhythmic risk.[55b] To date, work on hERG channel blockade has been a significant component of drug discovery within the pharmaceutical industry. The eight compounds with K_i σ_1 values of <15 nM and selectivities of >100-fold were evaluated the ability to block hERG through electrophysiological patch-clamp measurements. As shown in Table 6, compounds **54**, **71**, and **72** exhibited

DOI: 10.1021/acs.jmedchem.5b01416
J. Med. Chem. XXXX, XXX, XXX−XXX

lower affinities for hERG than did the others (IC_{50} > 2000 nM).

Table 6. Additional Data for Compounds Complying with K_i σ_1 < 15 nM and Selectivity of >100-Fold

compd	LD_{50} (mg/kg)[a]	hERG IC_{50} (μM)
53	754.5 (654.6−962.5)	1.45 ± 0.29
54	>2000	6.34 ± 0.60
59	900 (732.1−1762.5)	0.98 ± 0.1
60	780 (424.6−1586.2)	1.89 ± 0.3
65	717.3 (588.8−973.5)	1.61 ± 0.28
66	574.8 (453.2−769.2)	1.46 ± 0.18
71	1530 (1398.3−1809.2)	2.16 ± 0.24
72	1300 (948.5−1723.4)	2.68 ± 0.32

[a]95% confidence limits.

Acute Toxicity. The eight compounds that exhibited high affinities for the σ_1 receptor, with good selectivity compared to σ_2 receptor, were evaluated in terms of acute toxicity (LD_{50}) (Table 6). Compound **54** was nontoxic even at the highest dose tested (LD_{50} > 2000 mg/kg).

Functional Profile of the σ_1 Receptor. More recent studies using molecular biological tools have clearly demonstrated that σ_1 receptors and associated ligands modulate inositol 1,4,5-trisphosphate (IP3) receptors at the endoplasmic reticulum (ER) membrane. For example, the IP3 receptor-inhibiting protein, ankyrin, was found to be "removed" from IP3 receptors when σ_1 receptor agonists were applied to NG-108 cells, thus enhancing Ca^{2+} efflux from the ER into the cytosol.[56] The same results were observed by Wu and Bowen who found that the C-terminus portion of σ_1 receptors caused the dissociation of ankyrin from IP3 receptors in MCF-7 tumor cells.[57] In a study using CHO cells, Hayashi and Su found that σ_1 receptor agonists may activate σ_1 receptor by dissociating σ_1 receptors from binding-immunoglobulin protein (BiP), and σ_1 receptor antagonist did not affect the σ_1 receptor-BiP association and stabilized this complex.[58]

Recently, phenytoin-media shifts in σ_1 receptor ligand affinities and FRET-based biosensor studies of σ_1 receptor ligands have been used to categorize compounds as agonists or antagonists.[59] The functional activity of σ_1 receptor ligand was evaluated using phenytoin,[59a] a low potency allosteric modulator of σ_1 receptor that shifts known σ_1 receptor agonists to significantly higher affinities (K_i ratios without phenytoin vs with phenytoin of >1), while σ_1 receptor antagonists show small or no shift to lower affinity values (K_i ratios without phenytoin vs with phenytoin of ≤1). In such work, the functional activities of compound **54** with high-level σ_1 receptor-binding affinities, exhibiting greater selectivity for σ_1 receptor than σ_2 receptor, have been evaluated using phenytoin. Compound **54** afforded a small shift, lowering affinity when incubated in the presence of phenytoin (K_i ratio without vs with phenytoin, 0.73), thus acting antagonistically on the σ_1 receptor.

Formalin-Induced Nociceptive Behavior. Together, the data indicated that compounds **54**, **71**, and **72** had high affinities for σ_1 receptor, with good selectivities (compared to σ_2 receptor) together with low affinities for hERG and good safety profiles. These compounds were considered promising and were subjected to in vivo activity testing.

The classical model of acute and chronic pain, the formalin test, was performed to evaluate the antinociceptive effects. Intraplantar (ipl) injection of formalin elicits a biphasic pain response: early (phase I) and delayed (phase II), characterized by paw licking, biting, and other behaviors. Phase I pain is predominantly caused by direct activation of C-fibers, whereas phase II pain appears to be dependent on a combination of peripheral tissue inflammation and functional changes in the spinal cord, involving both peripheral and central sensitization.[60,61]

In the formalin test, pretreatment with compound **54** (80 mg/kg, ig) inhibited formalin-induced pain responses to a similar degree as 2, reducing licking and biting times in phase II to 45.88 ± 3.54 s and 41.16 ± 5.21 s, respectively. In contrast, the antiallodynic effects of compounds **71** and **72** attained statistical significance only when much higher doses (160 mg/kg, ig) were given, reducing licking and biting times to 59.65 ± 6.32 s and 56.43 ± 6.77 s, respectively.

To better characterize the antiallodynic effects of **54**, a wide range of doses was tested. Compound **54** (20−160 mg/kg) produced dose-dependent antinociception in phase II of the formalin test and was (slightly) more efficacious against delayed-phase pain (Figure 5). The ED_{50} value was 48.97 ± 3.89 mg/kg for phase II pain.

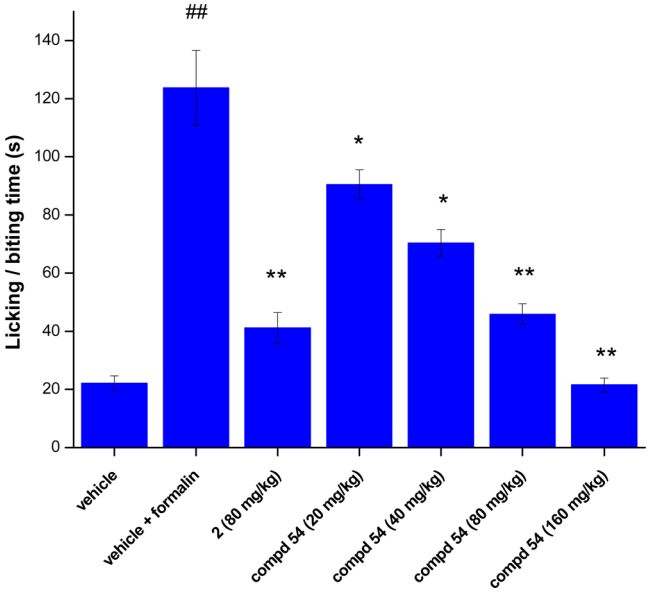

Figure 5. Antiallodynic effect of **2** and compound **54** in phase II (15−45 min) of the mice formalin test. Each column and vertical line represent the mean ± SEM of the values obtained in at least 10 animals. Statistically significant differences are the following: (#) p < 0.05, (##) p < 0.01 vs vehicle; (*) p < 0.05, (**) p < 0.01 vs vehicle + formalin (two-way ANOVA followed by Newman−Keuls test).

CCI (Chronic Constriction Injury) Model. Compound **54** was evaluated in a representative and frequently used model of neuropathic pain, the rat CCI model. Chronic constriction injury results in the development of allodynia- and spontaneous pain-like behaviors and hyperalgesia, which are normally maximal 10−14 days after surgery.[62,63] CCI rats exhibited signs of allodynia upon mechanical stimulation, and hyperalgesia to thermal stimulation; these are measures of neuropathic pain. Mechanical allodynia was quantified by measuring the hind-paw withdrawal response to von Frey hair stimulation, whereas thermal (heat) hyperalgesia was assessed using a

DOI: 10.1021/acs.jmedchem.5b01416
J. Med. Chem. XXXX, XXX, XXX−XXX

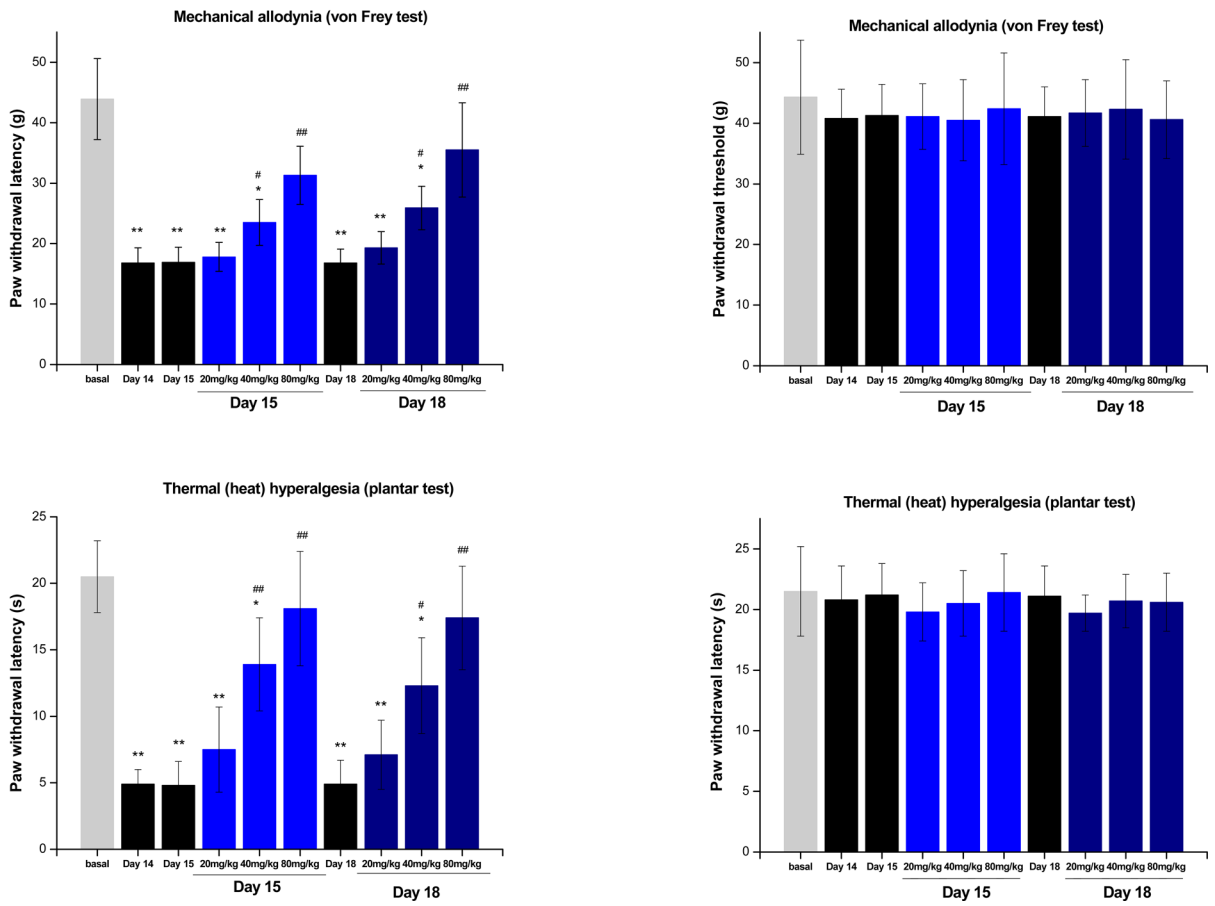

Figure 6. Antiallodynic effects of compound **54** on the expression of neuropathic pain in CCI and sham operated rats. Data are obtained from 10 rats per group and expressed as the mean ± SEM pressure threshold evoking paw withdrawal or latency to paw withdrawal. Statistically significant differences between the rats before surgery (basal) and surgery groups are the following: (∗) $p < 0.05$, (∗∗) $p < 0.01$ vs basal; (#) $p < 0.05$; (##) $p < 0.01$ vs vehicle treatment on days 14, 15, and 18 (two-way ANOVA followed by Newman−Keuls test).

plantar test; this was the hind-paw withdrawal latency in response to radiant heat.

As shown in Figure 6, compound **54** dose-dependently inhibited both mechanical allodynia and thermal hypersensitivity when given in a single dose (day 15) or in two doses (days 15 and 18); sham-operated rats exhibited no significant changes in mechanical or thermal sensitivity compared to those before surgery (the basal levels). The ED_{50} values after single dose treatment in terms of mechanical allodynia and thermal hypersensitivity were 51.88 ± 5.85 and 18.57 ± 2.32 mg/kg, respectively. For the double-dose treatment, the ED_{50} values were 40.26 ± 3.52 and 16.93 ± 2.17 mg/kg, respectively.

Motor Coordination: Rotarod Test. To investigate the possibility that the observed efficacy of compound **54** could interfere with motor coordination and thus with the response of mice in the nociceptive and neuropathic pain-related behavioral tests, motor performance was measured in the rotarod test.[41,42] As shown in Figure 7, no significant effect of compound **54** at an antiallodynic dose was observed and no treatment-related adverse effects were found. In contrast, **2** did a significant reduction in the permanence time on the rotating rod was observed at 80 mg/kg, after single intragastric administration.

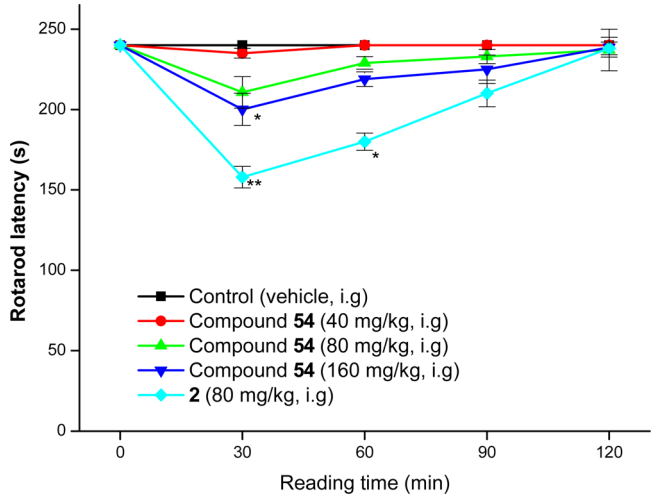

Figure 7. Dose−response effect of compounds **54** and **2** on motor coordination (rotarod test). Data are obtained from 8−10 mice per group and expressed as the mean ± SEM latency to fall down from rod. Statistically significant differences are the following: (∗) $p < 0.05$, (∗∗) $p < 0.01$ vs vehicle (two-way ANOVA followed by Newman−Keuls test).

DOI: 10.1021/acs.jmedchem.5b01416
J. Med. Chem. XXXX, XXX, XXX−XXX

Locomotor Activity Test. In the exploratory locomotor activity test, haloperidol (a known sedative)[64,65] served as a positive control. Pretreatment with 40, 80, and 160 mg/kg of compound **54** only mildly reduced exploratory locomotor activity (Table 7); in comparison, haloperidol significantly reduced spontaneous locomotor activity.

Table 7. Effects of Compound 54 and Haloperidol on the Spontaneous Locomotor Activity in Mice (Mean ± SD, n = 8)

compd	dose (mg/kg)	total distance (mm)
control		24881.4 ± 9545.8
haloperidol	0.1	23540.4 ± 7124.5
	0.3	8539.4 ± 5329.7*[a]
	1	1169.7 ± 662.3**[a]
control		24881.4 ± 9545.8
54	40	22826.6 ± 6293.7
	80	18282.4 ± 7050.5*[a]
	160	16458.3 ± 6260.3**[a]

[a](**) $p < 0.01$. (*) $p < 0.05$ vs control.

Pharmacokinetic Properties of Compound 54. We evaluated the in vitro and in vivo efficacies and the safety of compound **54** in rats (Table 8). Intravenous administration (5 mg/kg, n = 3) yielded detectable plasma levels, with a half-life ($t_{1/2}$) of 1.39 ± 0.18 h. Oral administration (80 mg/kg, n = 3) was associated with a $t_{1/2}$ of 2.88 ± 0.36 h. The area under the curve (AUC) was 956 ± 131 ng·h/mL after intravenous administration vs 13390 ± 1568 ng·h/mL after oral administration. After oral administration of 80 mg/mL, the peak serum concentration was 2923 ± 350 ng/mL and the T_{max} value 0.33 ± 0.04 h. The clearance was 49.3 ± 6.9 mL min^{-1} kg^{-1} in the intravenous administration. The bioavailability of compound **54** was 87.5%. Such encouraging preclinical data suggest that compound **54** has desirable drug-like human pharmacokinetic properties.

Selectivity Profile of Compound 54. To assess the interactions of compound **54** with other receptors or ion channels, a selectivity profile was created using additional receptors (including the μ-opioid, serotoninergic, H_3, cannabinoid, and NMDA receptors) and ion channels (voltage-gated sodium channel Nav 1.7 and the TRPV-1 protein) implicated in pain. Compound **54** showed no significant affinity (% inhibition at 1 μM of <50%) to any putative target (Supporting Information).

CONCLUSIONS

This detailed SAR investigation of pyridazinone scaffold derivatives reveals that several factors influence the binding affinity of these compounds to σ_1 and σ_2 receptor. The pyridazinone scaffold was crucial for activity, and a basic amine was necessary, matching the known σ_1 receptor pharmacophoric model. Piperidine was the preferred amino moiety (NRR), greatly improving σ_1 receptor binding affinity and maintaining selectivity. The aromatic group on the 2-position of the pyridazinone was essential for activity, and the introduction of halogens on the aromatic ring led to moderate affinities to σ_1 receptor and increased selectivity to σ_2 receptor.

In this study, a series of pyridazinone derivatives were synthesized via an efficient method, several of which were shown to be potent and selective σ_1 receptor ligands. Compound **54** appears safe in preliminary tests and exerts clear dose-dependent antiallodynic effects against formalin-induced pain in mice and antinociception (both mechanical allodynia and thermal hypersensitivity) in the rat CCI model. Moreover, compound **54** exhibited favorable pharmacokinetic properties and a good selective profile against other specific targets implicated in pain. Thus, compound **54** may facilitate the development of a novel class of candidate drugs for the treatment of neuropathic pain. Further studies of compound **54** and this series of derivatives are currently underway in our laboratory and will be reported in due course.

EXPERIMENTAL SECTION

Chemistry. All commercially available chemicals and reagents were used without further purification. Reagents were all of analytical grade or of chemical purity (>95%). Melting points were determined in open capillary tubes and are uncorrected. ^{1}H NMR spectra was recorded on a Bruker Avance III 600 spectrometer at 600 MHz (^{1}H) using $CDCl_3$ or DMSO-d_6 as solvent. Chemical shifts were given in δ values (ppm), using tetramethylsilane (TMS) as the internal standard; coupling constants (J) were given in Hz. Signal multiplicities were characterized as s (singlet), d (doublet), t (triplet), q (quartet), m (multiplet), br (broad signal). Analytical thin layer chromatography (TLC) was performed on silica gel GF254. Column chromatographic purification was carried out using silica gel. Compound purity is determined by high performance liquid chromatography (HPLC), and all final test compounds display purity higher than 95%. HPLC methods used the following: Agilent 1100 spectrometer; column, InertSustain C18 5.0 mm × 150 mm × 4.6 mm i.d. (SHIMADZU, Japan); mobile phase, 30 mmol NH_4COOH (ROE SCIENTIFIC INC, USA) aq/acetonitrile (Merck Company, Germany) 45/55; flow rate, 0.6 mL/min; column temperature, 40 °C. UV detection was performed at 210 nm.

6-Hydroxy-2-phenylpyridazin-3(2*H*)-one (8).[51b] Phenylhydrazine hydrochloride (**6**) (55 mmol) was added to maleic anhydride (**7**, 50 mmol), 400 mL of water, and 40 mL of concentrated hydrochloric acid solution. The mixture was heated at reflux for 9 h. After it was cooled, the resulting solid was collected by filtration, washed with ice−water. The solid was dissolved in saturated sodium bicarbonate solution; after filtration, the resulting filtrate was neutralized with 1 mol/L hydrochloric acid. The precipitate thus formed was filtered and washed with water. The resulting **8** was a white solid. Yield 79.8%; mp 272−273 °C; ^{1}H NMR (600 MHz, $CDCl_3$) δ 7.62 (d, J = 7.5 Hz, 2H), 7.52−7.47 (m, 2H), 7.43−7.38 (m, 1H), 7.10 (q, J = 9.8 Hz, 2H). A signal for the OH-proton is not visible.

General Procedure for the Preparation of Compounds 9 and 12−26. Method A. 2-Phenyl-6-(2-(piperidin-1-yl)ethoxy)-pyridazin-3(2*H*)-one(9). To a suspension of **8** (10 mmol) and 1-(2-chloroethyl)piperidine (10 mmol) in acetonitrile (100 mL), potassium carbonate (20 mmol) and a catalytic amount of potassium iodide (1% mol) were added. The resulting mixture was heated and refluxed for 6−8 h. The progress of the reaction was monitored by TLC. After filtering, the resulting filtrate was evaporated to dryness under reduced pressure. The residue was suspended in water (50 mL) and extracted with dichloromethane (3 × 25 mL). The combined organic layers were dried with anhydrous magnesium sulfate, the

Table 8. Plasma Pharmacokinetic Data after Administration of Compound 54 in Rats (n = 3/Group)

dose (mg/kg)	C_{max} (ng/mL)	T_{max} (h)	CL (mL min^{-1} kg^{-1})	$t_{1/2}$ (h)	AUC_{0-last} (ng·h/mL)	AUC_{0-inf} (ng·h/mL)	F (%)
80 (po)	2923 ± 350	0.33 ± 0.04		2.88 ± 0.36	11698 ± 1222	13390 ± 1568	87.5
5 (iv)			49.3 ± 6.9	1.39 ± 0.18	931 ± 125	956 ± 131	

DOI: 10.1021/acs.jmedchem.5b01416
J. Med. Chem. XXXX, XXX, XXX−XXX

filtrate evaporated under reduced pressure, and the crude product was purified by means of chromatography (10% MeOH/$CHCl_3$) to yield **9**. Pale yellow oil; yield 81.9%; ^{1}H NMR (600 MHz, $CDCl_3$) δ 7.67−7.65 (m, 2H), 7.43 (dd, J = 10.8, 5.1 Hz, 2H), 7.32 (t, J = 7.4 Hz, 1H), 7.02−6.95 (m, 2H), 4.28 (t, J = 5.9 Hz, 2H), 2.71 (t, J = 5.9 Hz, 2H), 2.46 (s, 4H), 1.63−1.53 (m, 4H), 1.45 (dd, J = 26.5, 5.0 Hz, 2H). HRMS (ESI) m/z 300.1713 (calcd 300.1707 for $C_{17}H_{22}N_3O_2$ $[M + H]^+$).

Method B. 6-(3-Bromopropoxy)-2-phenylpyridazin-3(2*H*)-one (10). To a solution of **8** (10 mmol) and 1,3-dibromopropane (20 mmol) in acetone (100 mL), potassium carbonate (20 mmol) was added, and the mixture was refluxed for 4−6 h. The progress of the reaction was monitored by TLC. After cooling to room temperature, the mixture was filtered and the solvent was evaporated under reduced pressure. The crude product was purified by means of chromatography (petroleum ether/EtOAc = 15/1) to yield **10**. Pale yellow oil; yield 61.7%; ^{1}H NMR (600 MHz, $CDCl_3$) δ 7.67 (dt, J = 8.7, 1.7 Hz, 2H), 7.49−7.44 (m, 2H), 7.38−7.33 (m, 1H), 7.08−6.99 (m, 2H), 4.32 (t, J = 5.9 Hz, 2H), 3.55 (t, J = 6.5 Hz, 2H), 2.30 (quintet, J = 6.2 Hz, 2H).

6-(4-Bromobutoxy)-2-phenylpyridazin-3(2*H*)-one (11). Pale yellow oil; yield 66.1%; ^{1}H NMR (600 MHz, $CDCl_3$) δ 7.67 (dt, J = 8.7, 1.7 Hz, 2H), 7.49−7.44 (m, 2H), 7.38−7.33 (m, 1H), 7.08−6.99 (m, 2H), 4.20 (t, J = 6.2 Hz, 2H), 3.47 (t, J = 6.6 Hz, 2H), 2.10−1.98 (m, 2H), 1.97−1.87 (m, 2H).

6-(3-Morpholinopropoxy)-2-phenylpyridazin-3(2*H*)-one (12). To a suspension of **10** (2 mmol) and morpholine (2.2 mmol), K_2CO_3 (4 mmol) in acetonitrile (50 mL) and a catalytic amount of KI (1% mol) were added, and the resulting mixture was refluxed for 6−8 h. After filtering, the resulting filtrate was evaporated to dryness under reduced pressure. The residue was suspended in water (10.0 mL) and extracted with dichloromethane (3 × 25 mL). The combined organic layers were dried with anhydrous magnesium sulfate, the filtrate evaporated under reduced pressure, and the crude product was purified by means of chromatography (10% MeOH/$CHCl_3$) to yield compound **12**. Pale yellow oil; yield 89.8%; ^{1}H NMR (600 MHz, $CDCl_3$) δ 7.65−7.63 (m, 2H), 7.45 (t, J = 7.9 Hz, 2H), 7.34 (t, J = 7.4 Hz, 1H), 7.02−6.95 (m, 2H), 4.32−4.17 (m, 2H), 3.77−3.57 (m, 4H), 2.80−2.62 (m, 1H), 2.53−2.42 (m, 5H), 2.00−1.88 (m, 2H). HRMS (ESI) m/z 316.1657 (calcd 316.1656 for $C_{17}H_{22}N_3O_3$ $[M + H]^+$).

2-Phenyl-6-(3-(piperidin-1-yl)propoxy)pyridazin-3(2*H*)-one (13). Pale yellow oil; yield 91.6%; ^{1}H NMR (600 MHz, $CDCl_3$) δ 7.65 (d, J = 1.1 Hz, 1H), 7.64 (s, 1H), 7.44 (dd, J = 10.8, 5.0 Hz, 2H), 7.35−7.30 (m, 1H), 7.00−6.94 (m, 2H), 4.19 (t, J = 6.4 Hz, 2H), 2.49−2.32 (m, 6H), 2.00−1.90 (m, 2H), 1.64−1.54 (m, 4H), 1.43 (s, 2H). HRMS (ESI) m/z 314.1872 (calcd 314.1863 for $C_{18}H_{24}N_3O_2$ $[M + H]^+$).

6-(3-(4-Methylpiperidin-1-yl)propoxy)-2-phenylpyridazin-3(2*H*)-one (14). Pale yellow oil; yield 88.3%; ^{1}H NMR (600 MHz, $CDCl_3$) δ 7.66 (d, J = 7.7 Hz, 2H), 7.44 (t, J = 7.9 Hz, 2H), 7.33 (t, J = 7.4 Hz, 1H), 7.01−6.95 (m, 2H), 4.20 (t, J = 6.4 Hz, 2H), 2.90 (d, J = 11.4 Hz, 2H), 2.52−2.39 (m, 2H), 2.01−1.85 (m, 4H), 1.66−1.56 (m, 2H), 1.41−1.30 (m, 1H), 1.24 (qd, J = 12.5, 3.6 Hz, 2H), 0.92 (d, J = 6.5 Hz, 3H). HRMS (ESI) m/z 328.2021 (calcd 328.2020 for $C_{19}H_{26}N_3O_2$ $[M + H]^+$).

6-(3-(3,5-Dimethylpiperidin-1-yl)propoxy)-2-phenylpyridazin-3(2*H*)-one(15). Pale yellow oil; yield 83.5%; ^{1}H NMR (600 MHz, $CDCl_3$) δ 7.68−7.60 (m, 2H), 7.42 (t, J = 7.0 Hz, 2H), 7.31 (t, J = 7.4 Hz, 1H), 7.00−6.93 (m, 2H), 4.23−4.15 (m, 2H), 2.97−2.87 (m, 2H), 2.59−2.51 (m, 2H), 2.01 (dd, J = 14.5, 7.1 Hz, 2H), 1.81−1.66 (m, 2H), 1.56 (t, J = 11.2 Hz, 2H), 0.83 (d, J = 6.6 Hz, 6H), 0.64−0.49 (m, 2H). HRMS (ESI) m/z 342.2180 (calcd 342.2176 for $C_{20}H_{28}N_3O_2$ $[M + H]^+$).

6-(3-(4-Oxopiperidin-1-yl)propoxy)-2-phenylpyridazin-3(2*H*)-one (16). Pale yellow oil; yield 84.1%; ^{1}H NMR (600 MHz, $CDCl_3$) δ 7.68−7.63 (m, 2H), 7.49−7.42 (m, 2H), 7.36−7.32 (m, 1H), 7.05−6.93 (m, 2H), 4.46−4.20 (m, 4H), 3.76−3.72 (m, 4H), 2.54−2.37 (m, 2H), 2.26−2.09 (m, 2H), 2.02−1.91 (m, 2H). HRMS (ESI) m/z 328.1663 (calcd 328.1656 for $C_{18}H_{22}N_3O_3$ $[M + H]^+$).

6-(3-(4-Methylpiperazin-1-yl)propoxy)-2-phenylpyridazin-3(2*H*)-one (17). Pale yellow oil; yield 82.9%; ^{1}H NMR (600 MHz, $CDCl_3$) δ 7.62 (dd, J = 8.5, 1.0 Hz, 2H), 7.43 (dd, J = 11.3, 4.6 Hz, 2H), 7.35−7.31 (m, 1H), 6.98 (q, J = 9.7 Hz, 2H), 4.19 (t, J = 6.3 Hz, 2H), 2.90−2.66 (m, 8H), 2.63−2.54 (m, 2H), 2.50 (s, 3H), 1.99−1.88 (m, 2H). HRMS (ESI) m/z 329.1980 (calcd 329.1972 for $C_{18}H_{25}N_4O_2$ $[M + H]^+$).

6-(3-(4-Ethylpiperazin-1-yl)propoxy)-2-phenylpyridazin-3(2*H*)-one (18). Pale yellow oil; yield 83.6%; ^{1}H NMR (600 MHz, $CDCl_3$) δ 7.61 (dd, J = 8.5, 1.0 Hz, 2H), 7.41 (t, J = 7.9 Hz, 2H), 7.33−7.29 (m, 1H), 7.01−6.93 (m, 2H), 4.39−4.10 (m, 2H), 2.81−2.39 (m, 12H), 2.02−1.81 (m, 2H), 1.14 (t, J = 7.3 Hz, 3H). HRMS (ESI) m/z 343.2135 (calcd 343.2129 for $C_{19}H_{27}N_4O_2$ $[M + H]^+$).

6-(3-(4-Methyl-1,4-diazepan-1-yl)propoxy)-2-phenylpyridazin-3(2*H*)-one (19). Pale yellow oil; yield 83.0%; ^{1}H NMR (600 MHz, $CDCl_3$) δ 7.68−7.65 (m, 2H), 7.49 (t, J = 7.4 Hz, 2H), 7.38 (t, J = 7.4 Hz, 1H), 7.05 (d, J = 9.9 Hz, 1H), 7.01 (d, J = 9.8 Hz, 1H), 4.25 (t, J = 6.2 Hz, 2H), 3.39−3.09 (m, 6H), 2.95 (t, J = 5.9 Hz, 2H), 2.82 (dd, J = 15.2, 8.0 Hz, 2H), 2.75 (s, 3H), 2.29 (s, 2H), 2.06−1.98 (m, 2H). HRMS (ESI) m/z 343.2131 (calcd 343.2129 for $C_{19}H_{27}N_4O_2$ $[M + H]^+$).

2-Phenyl-6-(3-(pyrrolidin-1-yl)propoxy)pyridazin-3(2*H*)-one (20). Pale yellow oil; yield 83.0%; ^{1}H NMR (600 MHz, $CDCl_3$) δ 7.69−7.65 (m, 2H), 7.47 (t, J = 7.8 Hz, 2H), 7.36 (t, J = 7.4 Hz, 1H), 7.08−6.94 (m, 2H), 4.24 (t, J = 6.4 Hz, 2H), 2.63−2.58 (m, 2H), 2.54 (t, J = 6.0 Hz, 4H), 2.02−1.95 (m, 2H), 1.85−1.73 (m, 4H). HRMS (ESI) m/z 300.1715 (calcd 300.1707 for $C_{17}H_{22}N_3O_2$ $[M + H]^+$).

6-(3-(Dimethylamino)propoxy)-2-phenylpyridazin-3(2*H*)-one (21). Pale yellow oil; yield 63.2%; ^{1}H NMR (600 MHz, $CDCl_3$) δ 7.66−7.59 (m, 2H), 7.47−7.41 (m, 2H), 7.37−7.31 (m, 1H), 7.07−6.98 (m, 2H), 4.32−4.20 (m, 2H), 3.24−3.17 (m, 2H), 2.80 (br, 6H), 2.35−2.21 (m, 2H). HRMS (ESI) m/z 274.1552 (calcd 274.1550 for $C_{15}H_{20}N_3O_2$ $[M + H]^+$).

6-(3-(Diethylamino)propoxy)-2-phenylpyridazin-3(2*H*)-one (22). Pale yellow oil; yield 66.0%; ^{1}H NMR (600 MHz, $CDCl_3$) δ 7.67−7.63 (m, 2H), 7.49−7.44 (m, 2H), 7.35 (dd, J = 10.7, 4.2 Hz, 1H), 7.04−6.98 (m, 2H), 4.25 (t, J = 6.1 Hz, 2H), 3.20−3.15 (m, 2H), 2.96−2.84 (m, 4H), 2.22−2.08 (m, 2H), 1.24 (t, J = 7.2 Hz, 6H). HRMS (ESI) m/z 302.1870 (calcd 302.1863 for $C_{17}H_{24}N_3O_2$ $[M + H]^+$).

6-(3-(Diisopropylamino)propoxy)-2-phenylpyridazin-3(2*H*)-one (23). Pale yellow oil; yield 64.0%; ^{1}H NMR (600 MHz, $CDCl_3$) δ 7.63 (d, J = 7.6 Hz, 2H), 7.37 (t, J = 7.9 Hz, 2H), 7.25 (t, J = 7.4 Hz, 1H), 6.96−6.86 (m, 2H), 4.15 (t, J = 6.4 Hz, 2H), 2.49 (t, J = 7.1 Hz, 2H), 2.35−2.28 (m, 4H), 1.86−1.78 (m, 2H), 1.44−1.32 (m, 4H), 0.80 (t, J = 7.4 Hz, 6H). HRMS (ESI) m/z 330.2181 (calcd 330.2176 for $C_{19}H_{28}N_3O_2$ $[M + H]^+$).

6-(4-(4-Piperidin-1-yl)butoxy)-2-phenylpyridazin-3(2*H*)-one (24). Pale yellow oil; yield 79.7%; ^{1}H NMR (600 MHz, $CDCl_3$) δ 7.65 (d, J = 7.6 Hz, 2H), 7.48 (t, J = 8.2 Hz, 2H), 7.33 (t, J = 7.3 Hz, 1H), 7.05−7.02 (m, 2H), 4.25−4.21 (m, 2H), 3.15−3.06 (m, 2H), 2.97−2.88 (m, 2H), 2.78−2.70 (m, 2H), 1.82−1.75 (m, 2H), 1.71−1.57 (m, 4H), 1.38−1.6 (m, 2H), 1.30−1.22 (m, 2H). HRMS (ESI) m/z 328.2029 (calcd 328.2020 for $C_{19}H_{26}N_3O_2$ $[M + H]^+$).

6-(4-(4-Methylpiperidin-1-yl)butoxy)-2-phenylpyridazin-3(2*H*)-one (25). Pale yellow oil; yield 82.3%; ^{1}H NMR (600 MHz, $CDCl_3$) δ 7.63 (d, J = 7.6 Hz, 2H), 7.37 (t, J = 7.9 Hz, 2H), 7.25 (t, J = 7.4 Hz, 1H), 6.96−6.86 (m, 2H), 4.19 (t, J = 6.4 Hz, 2H), 2.91 (d, J = 11.4 Hz, 2H), 2.41−2.32 (m, 2H), 1.93 (dd, J = 20.6, 8.6 Hz, 2H), 1.82−1.75 (m, 2H), 1.71−1.57 (m, 4H), 1.38−1.6 (m, 1H), 1.30−1.22 (m, 2H), 0.93 (d, J = 6.5 Hz, 3H). HRMS (ESI) m/z 342.2179 (calcd 342.2176 for $C_{20}H_{28}N_3O_2$ $[M + H]^+$).

6-(4-(3,5-Dimethylpiperidin-1-yl)butoxy)-2-phenylpyridazin-3(2*H*)-one (26). Pale yellow oil; yield 83.0%; ^{1}H NMR (600 MHz, $CDCl_3$) δ 7.64 (d, J = 7.6 Hz, 2H), 7.38 (t, J = 7.9 Hz, 2H), 7.25 (t, J = 7.4 Hz, 1H), 6.97−6.88 (m, 2H),4.29−4.16 (m, 2H), 4.16−4.10 (m, 2H), 3.10 (t, J = 20.3 Hz, 2H), 2.74−2.64 (m, 4H), 2.07−1.86 (m, 4H), 1.85−1.61 (m, 2H), 0.97 (d, J = 8.9 Hz, 3H), 0.83 (d, J = 6.6 Hz, 3H). HRMS (ESI) m/z 356.2340 (calcd 356.2333 for $C_{21}H_{30}N_3O_2$ $[M + H]^+$).

General Procedures for the Preparation of Intermediates 27−38. 6-Hydroxy-2-(*p*-tolyl)pyridazin-3(2*H*)-one (27). *p*-Tolylhydrazine hydrochloride (55 mmol) was added to maleic anhydride

DOI: 10.1021/acs.jmedchem.5b01416
J. Med. Chem. XXXX, XXX, XXX−XXX

(7, 50 mmol), 400 mL of water, and 40 mL of concentrated hydrochloric acid solution. The mixture was heated at reflux for 9 h. After it was cooled, the resulting solid was collected by filtration, washed with ice−water. The solid was dissolved in saturated sodium bicarbonate solution. After filtration, the resulting filtrate was neutralized with 1 mol/L hydrochloric acid. The precipitate thus formed was filtered and washed with water. The resulting **27** was a white solid. Yield 80.4%; mp 242−243 °C; ^{1}H NMR (600 MHz, $CDCl_3$) δ 7.47 (d, J = 8.3 Hz, 2H), 7.27 (d, J = 8.2 Hz, 2H), 7.13−7.04 (m, 2H), 2.42 (s, 3H). A signal for the OH-proton is not visible.

6-Hydroxy-2-(naphthalen-2-yl)pyridazin-3(2*H*)-one (28). White solid; yield 78.1%; mp 268−269 °C; ^{1}H NMR (600 MHz, $CDCl_3$) δ 8.14 (s, 1H), 7.94 (d, J = 8.9 Hz, 1H), 7.89 (s, 1H), 7.73 (d, J = 6.9 Hz, 1H), 7.57−7.52 (m, 2H), 7.46 (s, 1H), 7.17−7.09 (m, 2H). A signal for the OH-proton is not visible.

2-(4-Fluorophenyl)-6-hydroxypyridazin-3(2*H*)-one (29). White solid; yield 80.5%; mp 279−281 °C; ^{1}H NMR (600 MHz, $CDCl_3$) δ 7.69−7.64 (m, 2H), 7.12−7.09 (m, 2H), 7.03−6.99 (q, J = 9.7 Hz, 2H). A signal for the OH-proton is not visible.

2-(4-Chlorophenyl)-6-hydroxypyridazin-3(2*H*)-one (30). White solid; yield 83.0%; mp 281−282 °C; ^{1}H NMR (600 MHz, $CDCl_3$) δ 7.62 (d, J = 8.8 Hz, 2H), 7.47−7.43 (m, 2H), 7.10 (d, J = 8.5 Hz, 2H). A signal for the OH-proton is not visible.

2-(3,4-Dichlorophenyl)-6-hydroxypyridazin-3(2*H*)-one (31). Pale yellow solid; yield 76.2%; mp 291−292 °C; ^{1}H NMR (600 MHz, $CDCl_3$) δ 7.90 (d, J = 2.5 Hz, 1H), 7.65 (dd, J = 8.7, 2.5 Hz, 1H), 7.52 (d, J = 8.7 Hz, 1H), 7.01(br, 2H). A signal for the OH-proton is not visible.

2-(2,3-Dichlorophenyl)-6-hydroxypyridazin-3(2*H*)-one (32). Pale yellow solid; yield 77.9%; mp 289−292 °C; ^{1}H NMR (600 MHz, DMSO-d_6) δ 11.50 (s, 1H), 7.77 (dd, J = 8.1, 1.6 Hz, 1H), 7.58 (dd, J = 7.9, 1.6 Hz, 1H), 7.52 (t, J = 8.0 Hz, 1H), 7.25 (d, J = 9.9 Hz, 1H), 7.08 (d, J = 9.9 Hz, 1H).

2-(3,5-Dichlorophenyl)-6-hydroxypyridazin-3(2*H*)-one (33). Pale yellow solid; yield 74.8%; mp 288−289 °C; ^{1}H NMR (600 MHz, DMSO-d_6) δ 11.54 (s, 1H), 7.79 (d, J = 1.9 Hz, 2H), 7.62 (t, J = 1.9 Hz, 1H), 7.21 (d, J = 9.8 Hz, 1H), 7.05 (d, J = 9.8 Hz, 1H).

2-(2,4-Dichlorophenyl)-6-hydroxypyridazin-3(2*H*)-one (34). Pale yellow solid; yield 76.9%; mp 279−281 °C; ^{1}H NMR (600 MHz, DMSO-d_6) δ 11.49 (s, 1H), 7.85 (d, J = 2.0 Hz, 1H), 7.65−7.55 (m, 2H), 7.24 (d, J = 9.9 Hz, 1H), 7.06 (d, J = 9.9 Hz, 1H).

2-(2,5-Dichlorophenyl)-6-hydroxypyridazin-3(2*H*)-one (35). Pale yellow solid; yield 75.3%; mp 282−284 °C; ^{1}H NMR (600 MHz, DMSO) δ 11.48 (s, 1H), 7.78 (d, J = 2.5 Hz, 1H), 7.69 (d, J = 8.7 Hz, 1H), 7.60 (dd, J = 8.7, 2.5 Hz, 1H), 7.24 (d, J = 9.9 Hz, 1H), 7.07 (d, J = 9.9 Hz, 1H).

2-(3-Chloro-4-fluorophenyl)-6-hydroxypyridazin-3(2*H*)-one (36). Pale yellow solid; yield 76.8%; mp 291−292 °C; ^{1}H NMR (600 MHz, DMSO-d_6) δ 11.54 (s, 1H), 7.54−7.44 (m, 2H), 7.29 (tt, J = 9.2, 2.4 Hz, 1H), 7.20 (d, J = 9.8 Hz, 1H), 7.09−7.03 (m, 1H).

2-(3,4-Difluorophenyl)-6-hydroxypyridazin-3(2*H*)-one (37). Pale yellow solid; yield 78.6%; mp 285−287 °C; ^{1}H NMR (600 MHz, DMSO-d_6) δ 11.48 (s, 1H), 7.78−7.75 (m, 1H), 7.59−7.49 (m, 2H), 7.22 (d, J = 9.8 Hz, 1H), 7.05 (d, J = 9.8 Hz, 1H).

2-Cyclopentyl-6-hydroxypyridazin-3(2*H*)-one (38). Pale white solid; yield 55.9%; mp 231−232 °C; ^{1}H NMR (600 MHz, $CDCl_3$) δ 7.06 (d, J = 9.5 Hz, 2H), 5.44−5.25 (m, 1H), 1.93 (t, J = 31.1 Hz, 2H), 1.85−1.70 (m, 4H), 1.58−1.54 (m, 2H). A signal for the OH-proton is not visible.

General Procedures for the Preparation of Intermediates 39−49. 6-(3-Bromopropoxy)-2-(*p*-tolyl)pyridazin-3(2*H*)-one (39). To a solution of **27** (10 mmol) and 1,3-dibromopropane (20 mmol) in acetone (100 mL), potassium carbonate (20 mmol) was added, and the mixture was refluxed for 4−6 h. The progress of the reaction was monitored by TLC. After cooling to room temperature, the mixture was filtered and the solvent was evaporated under reduced pressure. The crude product was purified by means of chromatography (petroleum ether/EtOAc = 15/1) to yield compound **39**. Pale yellow oil; yield 75.4%; ^{1}H NMR (600 MHz, $CDCl_3$) δ 7.54 (d, J = 8.4 Hz, 2H), 7.27 (d, J = 8.2 Hz, 2H), 7.06−6.96 (m, 2H), 4.31 (t, J = 5.9 Hz, 2H), 3.55 (t, J = 6.5 Hz, 2H), 2.36 (s, 3H), 2.29 (quintet, J = 6.2 Hz, 2H).

6-(3-Bromopropoxy)-2-(naphthalen-2-yl)pyridazin-3(2*H*)-one (40). Pale yellow oil; yield 69.8%; ^{1}H NMR (600 MHz, $CDCl_3$) δ 8.23 (s, 1H), 7.94 (d, J = 8.9 Hz, 1H), 7.93−7.91 (m, 1H), 7.89−7.87 (m, 1H). 7.81 (dd, J = 8.8, 2.0 Hz, 1H), 7.56−7.49 (m, 2H), 7.07 (d, J = 9.7 Hz, 1H), 7.00 (d, J = 9.7 Hz, 1H), 4.35 (t, J = 5.9 Hz, 2H), 3.56 (t, J = 6.5 Hz, 2H), 2.36−2.24 (m, 2H).

6-(3-Bromopropoxy)-2-(4-fluorophenyl)pyridazin-3(2*H*)-one (41). Pale yellow oil; yield 65.3%; ^{1}H NMR (600 MHz, $CDCl_3$) δ 7.69−7.64 (m, 2H), 7.15−7.11 (m, 2H), 7.02−6.98 (m, 2H), 4.31 (t, J = 5.9 Hz, 2H), 3.55 (t, J = 6.5 Hz, 2H), 2.30 (quintet, J = 6.2 Hz, 2H).

6-(3-Bromopropoxy)-2-(4-chlorophenyl)pyridazin-3(2*H*)-one (42). Pale yellow solid; yield 71.0%; mp 79−81 °C; ^{1}H NMR (600 MHz, $CDCl_3$) δ 7.67 (d, J = 8.7 Hz, 2H), 7.42 (d, J = 8.7 Hz, 2H), 7.04−6.97 (m, 2H), 4.32 (t, J = 5.9 Hz, 2H), 3.55 (t, J = 6.4 Hz, 2H), 2.30 (quintet, J = 6.1 Hz, 2H).

6-(3-Bromopropoxy)-2-(3,4-dichlorophenyl)pyridazin-3(2*H*)-one (43). Pale yellow solid; yield 71.8%; mp 83−85 °C; ^{1}H NMR (600 MHz, $CDCl_3$) δ 7.90 (d, J = 2.5 Hz, 1H), 7.65 (dd, J = 8.7, 2.5 Hz, 1H), 7.52 (d, J = 8.7 Hz, 1H), 7.01(s, 2H), 4.34 (t, J = 5.9 Hz, 2H), 3.57 (t, J = 6.4 Hz, 2H), 2.32 (quintet, J = 6.2 Hz, 2H).

6-(3-Bromopropoxy)-2-(2,3-dichlorophenyl)pyridazin-3(2*H*)-one (44). Pale yellow solid; yield 71.3%; mp 53−55 °C; ^{1}H NMR (600 MHz, $CDCl_3$) δ 7.57 (dd, J = 6.5, 3.1 Hz, 1H), 7.40−7.32 (m, 2H), 7.09−7.03 (m, 2H), 4.25 (t, J = 5.9 Hz, 2H), 3.55 (t, J = 6.5 Hz, 2H), 2.60−1.94 (m, 2H).

6-(3-Bromopropoxy)-2-(3,5-dichlorophenyl)pyridazin-3(2*H*)-one (45). Pale yellow solid; yield 71.3%; mp 63−64 °C; ^{1}H NMR (600 MHz, $CDCl_3$) δ 7.72 (d, J = 1.9 Hz, 2H), 7.35 (t, J = 1.9 Hz, 1H), 7.11−6.96 (m, 2H), 4.35 (t, J = 5.9 Hz, 2H), 3.58 (t, J = 6.4 Hz, 2H), 2.36−2.31 (m, 2H).

6-(3-Bromopropoxy)-2-(2,4-dichlorophenyl)pyridazin-3(2*H*)-one (46). Pale yellow oil; yield 70.1%; ^{1}H NMR (600 MHz, $CDCl_3$) δ 7.55 (dd, J = 1.5, 1.0 Hz, 1H), 7.42−7.35 (m, 2H), 7.08−7.01 (m, 2H), 4.24 (t, J = 5.9 Hz, 2H), 3.53 (t, J = 6.5 Hz, 2H), 2.28 (p, J = 6.2 Hz, 2H).

6-(3-Bromopropoxy)-2-(2,5-dichlorophenyl)pyridazin-3(2*H*)-one (47). Pale yellow oil; yield 71.8%; ^{1}H NMR (600 MHz, $CDCl_3$) δ 7.49 (d, J = 8.6 Hz, 1H), 7.46 (d, J = 2.4 Hz, 1H), 7.39 (dd, J = 8.6, 2.4 Hz, 1H), 7.09−7.03 (m, 2H), 4.27 (t, J = 5.9 Hz, 2H), 3.55 (t, J = 6.5 Hz, 2H), 2.31−2.28 (m, 2H).

6-(3-Bromopropoxy)-2-(3-chloro-4-fluorophenyl)pyridazin-3(2*H*)-one (48). Pale yellow solid; yield 74.8%; mp 73−75 °C; ^{1}H NMR (600 MHz, $CDCl_3$) δ 7.53−7.37 (m, 2H), 7.07−6.96 (m, 2H), 6.81 (tt, J = 8.7, 2.3 Hz, 1H), 4.36 (t, J = 5.9 Hz, 2H), 3.58 (t, J = 6.4 Hz, 2H), 2.37−2.31 (m, 2H).

6-(3-Bromopropoxy)-2-(3,4-difluorophenyl)pyridazin-3(2*H*)-one (49). Pale yellow solid; yield 69.9%; mp 43−45 °C; ^{1}H NMR (600 MHz, $CDCl_3$) δ 7.66−7.63 (m, 1H), 7.55−7.52 (m, 1H), 7.24 (dd, J = 18.5, 8.9 Hz, 1H), 7.05−6.97 (m, 2H), 4.34 (t, J = 5.9 Hz, 2H), 3.57 (t, J = 6.4 Hz, 2H), 2.36−2.28 (m, 2H).

General Procedures for the Synthesis of Compounds 50−61. Method B. 6-(3-(Piperidin-1-yl)propoxy)-2-(*p*-tolyl)-pyridazin-3(2*H*)-one (50). To a suspension of **39** (2 mmol) and piperidine (2.2 mmol), K_2CO_3 (4 mmol) in acetonitrile (50 mL) and a catalytic amount of KI (1% mol) were added, and the resulting mixture was refluxed for 6−8 h. After filtering, the resulting filtrate was evaporated to dryness under reduced pressure. The residue was suspended in water (10.0 mL) and extracted with dichloromethane (3 × 25 mL). The combined organic layers were dried with anhydrous magnesium sulfate, the filtrate was evaporated under reduced pressure, and the crude product was purified by means of chromatography (10% MeOH/$CHCl_3$) to yield compound **50**. Pale yellow oil; yield 81.5%; ^{1}H NMR (600 MHz, $CDCl_3$) δ 7.48 (d, J = 8.3 Hz, 2H), 7.22 (d, J = 8.1 Hz, 2H), 6.98−6.93 (m, 2H), 4.17 (t, J = 6.2 Hz, 2H), 2.59 (dd, J = 18.2, 10.4 Hz, 6H), 2.35 (s, 3H), 2.09−1.97 (m, 2H), 1.71−1.61 (m, 4H), 1.46 (s, 2H). HRMS (ESI) m/z 328.2027(calcd 328.2020 for $C_{19}H_{26}N_3O_2$ $[M + H]^+$).

2-(Naphthalen-2-yl)-6-(3-(piperidin-1-yl)propoxy)pyridazin-3(2*H*)-one (51). Pale yellow oil; yield 87.2%; ^{1}H NMR (600 MHz,

DOI: 10.1021/acs.jmedchem.5b01416
J. Med. Chem. XXXX, XXX, XXX−XXX

$CDCl_3$) δ 8.20 (d, J = 1.7 Hz, 1H), 7.95−7.85 (m, 3H), 7.79 (dd, J = 8.8, 2.1 Hz, 1H), 7.54−7.49 (m, 2H), 7.03 (dd, J = 22.4, 9.7 Hz, 2H), 4.25 (t, J = 6.4 Hz, 2H), 2.45 (dd, J = 24.5, 16.7 Hz, 6H), 2.05−1.92 (m, 2H), 1.66−1.55 (m, 4H), 1.45 (s, 2H). HRMS (ESI) *m/z* 364.2026(calcd 364.2020 for $C_{22}H_{26}N_3O_2$ $[M + H]^+$).

2-(4-Fluorophenyl)-6-(3-(piperidin-1-yl)propoxy)pyridazin-3(2*H*)-one (52). Pale yellow oil; yield 80.6%; ^1H NMR (600 MHz, $CDCl_3$) δ 7.65−7.61 (m, 2H), 7.14−7.07 (m, 2H), 6.99 (d, J = 9.7 Hz, 2H), 4.20 (t, J = 6.2 Hz, 2H), 2.66 (dd, J = 17.3, 9.3 Hz, 6H), 2.15−2.00 (m, 2H), 1.75−1.68 (m, 4H), 1.50 (s, 2H). HRMS (ESI) *m/z* 332.1775 (calcd 332.1769 for $C_{18}H_{23}FN_3O_2$ $[M + H]^+$).

2-(4-Chlorophenyl)-6-(3-(piperidin-1-yl)propoxy)pyridazin-3(2*H*)-one (53). Pale yellow solid; yield 86.7%; mp 91−92 °C; ^1H NMR (600 MHz, $CDCl_3$) δ 7.68−7.64 (m, 2H), 7.42−7.38 (m, 2H), 6.97 (s, 2H), 4.20 (t, J = 6.4 Hz, 2H), 2.42 (dd, J = 22.1, 14.4 Hz, 6H), 2.04−1.86 (m, 2H), 1.65−1.53 (m, 4H), 1.43 (s, 2H). HRMS (ESI) *m/z* 348.1477(calcd 348.1473 for $C_{18}H_{23}ClN_3O_2$ $[M + H]^+$).

2-(3,4-Dichlorophenyl)-6-(3-(piperidin-1-yl)propoxy)-pyridazin-3(2*H*)-one (54). Pale yellow solid; yield 88.4%; mp 61−62 °C; ^1H NMR (600 MHz, $CDCl_3$) δ 7.88 (d, J = 2.4 Hz, 1H), 7.65 (dd, J = 8.7, 2.5 Hz, 1H), 7.50 (d, J = 8.7 Hz, 1H), 7.04−6.96 (m, 2H), 4.22 (t, J = 6.4 Hz, 2H), 2.53−2.38 (m, 6H), 2.02−1.92 (m, 2H), 1.66−1.58 (m, 4H), 1.45 (br, 2H). HRMS (ESI) *m/z* 382.1087 (calcd 382.1084 for $C_{18}H_{22}Cl_2N_3O_2$ $[M + H]^+$).

2-(2,3-Dichlorophenyl)-6-(3-(piperidin-1-yl)propoxy)-pyridazin-3(2*H*)-one (55). Pale yellow oil; yield 81.5%; ^1H NMR (600 MHz, $CDCl_3$) δ 7.59−7.52 (m, 1H), 7.37−7.32 (m, 2H), 7.07−6.98 (m, 2H), 4.13 (t, J = 6.3 Hz, 2H), 2.43−2.38 (m, 6H), 1.99−1.87 (m, 2H), 1.65−1.49 (m, 4H), 1.43 (s, 2H). HRMS (ESI) *m/z* 382.1088 (calcd 382.1084 for $C_{18}H_{22}Cl_2N_3O_2$ $[M + H]^+$).

2-(3,5-Dichlorophenyl)-6-(3-(piperidin-1-yl)propoxy)-pyridazin-3(2*H*)-one (56). Pale yellow oil; yield 82.1%; ^1H NMR (600 MHz, $CDCl_3$) δ 7.70 (d, J = 1.9 Hz, 2H), 7.32 (t, J = 1.9 Hz, 1H), 6.99 (d, J = 1.1 Hz, 2H), 4.22 (t, J = 6.4 Hz, 2H), 2.47−2.41 (m, 6H), 2.03−1.93 (m, 2H), 1.63−1.56 (m, 4H), 1.45 (br, 2H). HRMS (ESI) *m/z* 382.1079 (calcd 382.1084 for $C_{18}H_{22}Cl_2N_3O_2$ $[M + H]^+$).

2-(2,4-Dichlorophenyl)-6-(3-(piperidin-1-yl)propoxy)-pyridazin-3(2*H*)-one (57). Pale yellow oil; yield 83.2%; ^1H NMR (600 MHz, $CDCl_3$) δ 7.55 (d, J = 1.6 Hz, 1H), 7.41−7.34 (m, 2H), 7.02 (q, J = 9.9 Hz, 2H), 4.13 (t, J = 6.5 Hz, 2H), 2.44−2.39 (m, 6H), 2.00−1.87 (m, 2H), 1.66−1.52 (m, 4H), 1.44 (br, 2H). HRMS (ESI) *m/z* 382.1086 (calcd 382.1084 for $C_{18}H_{22}Cl_2N_3O_2$ $[M + H]^+$).

2-(2,5-Dichlorophenyl)-6-(3-(piperidin-1-yl)propoxy)-pyridazin-3(2*H*)-one (58). Pale yellow oil; yield 85.3%; ^1H NMR (600 MHz, $CDCl_3$) δ 7.47 (d, J = 8.6 Hz, 1H), 7.44 (d, J = 2.4 Hz, 1H), 7.37 (dd, J = 8.6, 2.5 Hz, 1H), 7.03 (q, J = 9.9 Hz, 2H), 4.15 (t, J = 6.5 Hz, 2H), 2.44−2.39 (m, 6H), 2.01−1.88 (m, 2H), 1.63−1.52 (m, 4H), 1.44 (br, 2H). HRMS (ESI) *m/z* 382.1088 (calcd 382.1084 for $C_{18}H_{22}Cl_2N_3O_2$ $[M + H]^+$).

2-(3-Chloro-4-fluorophenyl)-6-(3-(piperidin-1-yl)propoxy)-pyridazin-3(2*H*)-one (59). Pale yellow oil; yield 81.6%; ^1H NMR (600 MHz, $CDCl_3$) δ 7.50−7.38 (m, 2H), 7.07−6.93 (m, 2H), 6.80−6.75 (m, 1H), 4.23 (t, J = 6.4 Hz, 2H), 2.47−2.40 (m, 6H), 2.03−1.90 (m, 2H), 1.67−1.54 (m, 4H), 1.44 (br, 2H). HRMS (ESI) *m/z* 366.1381 (calcd 366.1379 for $C_{18}H_{22}ClFN_3O_2$ $[M + H]^+$).

2-(3,4-Difluorophenyl)-6-(3-(piperidin-1-yl)propoxy)-pyridazin-3(2*H*)-one (60). Pale yellow oil; yield 82.4%; ^1H NMR (600 MHz, $CDCl_3$) δ 7.64−7.60 (m, 1H), 7.55−7.45 (m, 1H), 7.21 (dd, J = 18.5, 8.9 Hz, 1H), 7.03−6.93 (m, 2H), 4.20 (t, J = 6.4 Hz, 2H), 2.45−2.39 (m, 6H), 2.01−1.91 (m, 2H), 1.64−1.51 (m, 4H), 1.44 (d, J = 4.6 Hz, 2H). HRMS (ESI) *m/z* 350.1682 (calcd 350.1675 for $C_{18}H_{22}F_2N_3O_2$ $[M + H]^+$).

Method A: 2-Cyclopentyl-6-(3-(piperidin-1-yl)propoxy)-pyridazin-3(2*H*)-one (61). To a suspension of **38** (10 mmol) and 1-(3-chloropropyl)piperidine (10 mmol) in acetonitrile (100 mL), potassium carbonate (20 mmol) and a catalytic amount of potassium iodide (1% mol) were added. The resulting mixture was heated and refluxed for 8 h. The progress of the reaction was monitored by TLC. After filtering, the resulting filtrate was evaporated to dryness under reduced pressure. The residue was suspended in water (50 mL) and extracted with dichloromethane (3 × 25 mL). The combined organic layers were dried with anhydrous magnesium sulfate, the filtrate was evaporated under reduced pressure, and the crude product was purified by means of chromatography (10% MeOH/$CHCl_3$) to yield **61**. Pale yellow oil; yield 64.6%; ^1H NMR (600 MHz, $CDCl_3$) δ 6.67−6.50 (m, 2H), 5.19−5.00 (m, 1H), 3.93 (dd, J = 14.8, 8.5 Hz, 2H), 2.19 (dd, J = 22.9, 15.5 Hz, 6H), 1.82−1.51 (m, 8H), 1.35 (dd, J = 23.9, 18.4 Hz, 6H), 1.18 (s, 2H). HRMS (ESI) *m/z* 306.2183 (calcd 306.2176 for $C_{17}H_{28}N_3O_2$ $[M + H]^+$).

General Procedures for the Synthesis of Compounds 62−72. Method B. 6-(3-(4-Methylpiperidin-1-yl)propoxy)-2-(*p*-tolyl)pyridazin-3(2*H*)-one (62). To a suspension of **39** (2 mmol) and 4-methylpiperidine (2.2 mmol), K_2CO_3 (4 mmol) in acetonitrile (50 mL) and a catalytic amount of KI (1% mol) were added, and the resulting mixture was refluxed for 6−8 h. After filtering, the resulting filtrate was evaporated to dryness under reduced pressure. The residue was suspended in water (10.0 mL) and extracted with dichloromethane (3 × 25 mL). The combined organic layers were dried with anhydrous magnesium sulfate, the filtrate was evaporated under reduced pressure, and the crude product was purified by means of chromatography (10% MeOH/$CHCl_3$) to yield compound **62**. Pale yellow oil; yield 82.9%; ^1H NMR (600 MHz, $CDCl_3$) δ 7.52 (d, J = 8.3 Hz, 2H), 7.23 (d, J = 8.2 Hz, 2H), 6.95 (q, J = 9.7 Hz, 2H), 4.18 (t, J = 6.4 Hz, 2H), 2.88 (d, J = 11.3 Hz, 2H), 2.45−2.42 (m, 2H), 2.37 (s, 3H), 1.97−1.86 (m, 4H), 1.60 (d, J = 12.8 Hz, 2H), 1.39−1.31 (m, 1H), 1.28−1.18 (m, 2H), 0.91 (d, J = 6.5 Hz, 3H). HRMS (ESI) *m/z* 342.2185(calcd 342.2176 for $C_{20}H_{28}N_3O_2$ $[M + H]^+$).

6-(3-(4-Methylpiperidin-1-yl)propoxy)-2-(naphthalen-2-yl)-pyridazin-3(2*H*)-one (63). Pale yellow oil; yield 81.3%; ^1H NMR (600 MHz, $CDCl_3$) δ 8.20 (d, J = 1.8 Hz, 1H), 7.89 (ddd, J = 16.8, 11.9, 6.1 Hz, 3H), 7.79 (dd, J = 8.8, 2.1 Hz, 1H), 7.54−7.47 (m, 2H), 7.03 (dd, J = 23.3, 9.7 Hz, 2H), 4.25 (t, J = 6.4 Hz, 2H), 2.90 (d, J = 11.4 Hz, 2H), 2.53−2.43 (m, 2H), 2.01−1.89 (m, 4H), 1.62 (d, J = 12.8 Hz, 2H), 1.43−1.18 (m, 3H), 0.93 (d, J = 6.5 Hz, 3H). HRMS (ESI) *m/z* 378.2180(calcd 378.2176 for $C_{23}H_{28}N_3O_2$ $[M + H]^+$).

2-(4-Fluorophenyl)-6-(3-(4-methylpiperidin-1-yl)propoxy)-pyridazin-3(2*H*)-one (64). Pale yellow oil; yield 81.9%; ^1H NMR (600 MHz, $CDCl_3$) δ 7.68−7.63 (m, 2H), 7.15−7.09 (m, 2H), 7.01−6.95 (m, 2H), 4.19 (t, J = 6.4 Hz, 2H), 2.88 (d, J = 11.1 Hz, 2H), 2.48−2.40 (m, 2H), 1.98−1.84 (m, 4H), 1.61 (d, J = 12.8 Hz, 2H), 1.35 (d, J = 6.0 Hz, 1H), 1.23 (q, J = 11.4 Hz, 2H), 0.91 (d, J = 6.5 Hz, 3H). HRMS (ESI) *m/z* 346.1933(calcd 346.1925 for $C_{19}H_{25}FN_3O_2$ $[M + H]^+$).

2-(4-Chlorophenyl)-6-(3-(4-methylpiperidin-1-yl)propoxy)-pyridazin-3(2*H*)-one (65). Pale yellow solid; yield 82.2%; mp 95−96 °C; ^1H NMR (600 MHz, $CDCl_3$) δ 7.68−7.65 (m, 2H), 7.43−7.39 (m, 2H), 7.01−6.96 (m, 2H), 4.21 (t, J = 6.4 Hz, 2H), 2.89 (d, J = 11.4 Hz, 2H), 2.49−2.43 (m, 2H), 1.99−1.87 (m, 4H), 1.62 (d, J = 12.9 Hz, 2H), 1.42−1.33 (m, 1H), 1.28−1.21 (m, 3.6 Hz, 2H), 0.92 (d, J = 6.5 Hz, 3H). HRMS (ESI) *m/z* 362.1633 (calcd 362.1630 for $C_{19}H_{25}ClN_3O_2$ $[M + H]^+$).

2-(3,4-Dichlorophenyl)-6-(3-(4-methylpiperidin-1-yl)-propoxy)pyridazin-3(2*H*)-one (66). Pale white solid; yield 83.7%; mp 54−56 °C; ^1H NMR (600 MHz, $CDCl_3$) δ 7.88 (d, J = 2.5 Hz, 1H), 7.65 (dd, J = 8.7, 2.5 Hz, 1H), 7.50 (d, J = 8.7 Hz, 1H), 6.99 (d, J = 10.0 Hz, 2H), 4.22 (t, J = 6.4 Hz, 2H), 2.91 (d, J = 11.4 Hz, 2H), 2.49−2.45 (m, 2H), 2.02−1.90 (m, 4H), 1.63 (d, J = 12.8 Hz, 2H), 1.29−1.22 (m, 3H), 0.93 (d, J = 6.5 Hz, 3H). HRMS (ESI) *m/z* 396.1246 (calcd 396.1240 for $C_{19}H_{24}Cl_2N_3O_2$ $[M + H]^+$).

2-(2,3-Dichlorophenyl)-6-(3-(4-methylpiperidin-1-yl)-propoxy)pyridazin-3(2*H*)-one (67). Pale yellow oil; yield 82.1%; ^1H NMR (600 MHz, $CDCl_3$) δ 7.61−7.52 (m, 1H), 7.38−7.30 (m, 2H), 7.04 (q, J = 9.9 Hz, 2H), 4.14 (t, J = 6.3 Hz, 2H), 2.88 (d, J = 11.5 Hz, 2H), 2.44 (t, J = 6.3 Hz, 2H), 2.00−1.85 (m, 4H), 1.61 (d, J = 13.0 Hz, 2H), 1.41−1.30 (m, 1H), 1.26−1.20 (m, 2H), 0.92 (d, J = 6.5 Hz, 3H). HRMS (ESI) *m/z* 396.1242 (calcd 396.1240 for $C_{19}H_{24}Cl_2N_3O_2$ $[M + H]^+$).

2-(3,5-Dichlorophenyl)-6-(3-(4-methylpiperidin-1-yl)-propoxy)pyridazin-3(2*H*)-one (68). Pale yellow oil; yield 81.3%; ^1H NMR (600 MHz, $CDCl_3$) δ 7.71 (d, J = 1.9 Hz, 2H), 7.34 (t, J = 1.9 Hz, 1H), 7.05−6.95 (m, 2H), 4.23 (t, J = 6.4 Hz, 2H), 2.91 (d, J =

DOI: 10.1021/acs.jmedchem.5b01416
J. Med. Chem. XXXX, XXX, XXX−XXX

11.5 Hz, 2H), 2.50−2.45 (m, 2H), 2.02−1.89 (m, 4H), 1.64 (d, J = 12.9 Hz, 2H), 1.44−1.32 (m, 1H), 1.30−1.20 (m, 2H), 0.94 (d, J = 6.5 Hz, 3H). HRMS (ESI) m/z 396.1243 (calcd 396.1240 for $C_{19}H_{24}Cl_2N_3O_2$ $[M + H]^+$).

2-(2,4-Dichlorophenyl)-6-(3-(4-methylpiperidin-1-yl)-propoxy)pyridazin-3(2*H*)-one (69). Pale yellow oil; yield 81.2%; ^{1}H NMR (600 MHz, $CDCl_3$) δ 7.56−7.54 (m, 1H), 7.40−7.33 (m, 2H), 7.02 (q, J = 9.9 Hz, 2H), 4.13 (t, J = 6.5 Hz, 2H), 2.88 (d, J = 11.5 Hz, 2H), 2.49−2.41 (m, 2H), 1.99−1.80 (m, 4H), 1.61 (d, J = 13.0 Hz, 2H), 1.43−1.29 (m, 1H), 1.29−1.15 (m, 2H), 0.92 (d, J = 6.5 Hz, 3H). HRMS (ESI) m/z 396.1248 (calcd 396.1240 for $C_{19}H_{24}Cl_2N_3O_2$ $[M + H]^+$).

2-(2,5-Dichlorophenyl)-6-(3-(4-methylpiperidin-1-yl)-propoxy)pyridazin-3(2*H*)-one (70). Pale yellow oil; yield 80.7%; ^{1}H NMR (600 MHz, $CDCl_3$) δ 7.47−7.44 (m, 1H), 7.43 (d, J = 2.4 Hz, 1H), 7.36 (dd, J = 8.6, 2.5 Hz, 1H), 7.08−6.98 (m, 2H), 4.14 (t, J = 6.5 Hz, 2H), 2.87 (d, J = 11.5 Hz, 2H), 2.47−2.37 (m, 2H), 1.98−1.85 (m, 4H), 1.60 (d, J = 13.5 Hz, 2H), 1.34 (ddd, J = 11.2, 6.9, 4.0 Hz, 1H), 1.22 (ddd, J = 15.5, 12.3, 3.7 Hz, 2H), 0.91 (d, J = 6.5 Hz, 3H). HRMS (ESI) m/z 396.1244 (calcd 396.1240 for $C_{19}H_{24}Cl_2N_3O_2$ $[M + H]^+$).

2-(3-Chloro-4-fluorophenyl)-6-(3-(4-methylpiperidin-1-yl)-propoxy)pyridazin-3(2*H*)-one (71). Pale yellow oil; yield 78.9%; ^{1}H NMR (600 MHz, $CDCl_3$) δ 7.55−7.39 (m, 2H), 7.00−6.97 (m, 2H), 6.80−6.75 (m, 1H), 4.23 (t, J = 6.4 Hz, 2H), 2.90 (d, J = 11.5 Hz, 2H), 2.56−2.41 (m, 2H), 2.02−1.86 (m, 4H), 1.71−1.57 (m, 2H), 1.39−1.33 (m, 1H), 1.27−1.21 (m, 2H), 0.92 (d, J = 6.5 Hz, 3H). HRMS (ESI) m/z 380.1542 (calcd 380.1536 for $C_{19}H_{24}ClFN_3O_2$ $[M + H]^+$).

2-(3,4-Difluorophenyl)-6-(3-(4-methylpiperidin-1-yl)-propoxy)pyridazin-3(2*H*)-one (72). Pale yellow oil; yield 79.3%; ^{1}H NMR (600 MHz, $CDCl_3$) δ 7.65−7.61 (m, 1H), 7.54−7.51 (m, 1H), 7.23 (dd, J = 18.4, 9.0 Hz, 1H), 7.05−6.96 (m, 2H), 4.22 (t, J = 6.4 Hz, 2H), 2.90 (d, J = 11.5 Hz, 2H), 2.50−2.41 (m, 2H), 2.05−1.84 (m, 4H), 1.63 (d, J = 13.1 Hz, 2H), 1.44−1.30 (m, 1H), 1.28−1.21 (m, 2H), 0.93 (d, J = 6.5 Hz, 3H). HRMS (ESI) m/z 364.1838 (calcd 364.1831 for $C_{19}H_{24}F_2N_3O_2$ $[M + H]^+$).

General Procedures for the Preparation of Intermediates 73−75. 2-(3,4-Dichlorophenyl)-6-hydroxy-4,5-dimethylpyridazin-3(2*H*)-one (73). 3,4-Dicholrophenylhydrazine hydrochloride (55 mmol) was added to 3,4-dimethylfuran-2,5-dione (50 mmol), 400 mL of water, and 40 mL of 35% hydrochloric acid solution. The mixture was heated at reflux for 9 h. After it was cooled, the resulting solid was collected by filtration, washed with ice−water. The solid was dissolved in saturated sodium bicarbonate solution, and after filtration, the resulting filtrate was neutralized with 1 mol/L hydrochloric acid. The precipitate thus formed was filtered and washed with water. The resulting **73** was a white solid. Yield 77.4%; mp 255−257 °C; ^{1}H NMR (600 MHz, DMSO-d_6) δ 11.42 (s, 1H), 7.97 (d, J = 2.4 Hz, 1H), 7.74−7.59 (m, 2H), 2.09 (s, 6H).

2-(3,4-Dichlorophenyl)-4-hydroxy-5,6,7,8-tetrahydrophthalazin-1(2*H*)-one (74). Pale yellow solid; yield 79.1%; mp 261−263 °C; ^{1}H NMR (600 MHz, DMSO-d_6) δ 11.41 (s, 1H), 7.97 (d, J = 2.4 Hz, 1H), 7.71 (dt, J = 8.8, 5.6 Hz, 2H), 3.35 (s, 2H), 2.56−2.46 (m, 2H), 2.44 (s, 2H), 1.69 (s, 2H).

2-(3,4-Dichlorophenyl)-4-hydroxyphthalazin-1(2*H*)-one (75). Pale yellow solid; yield 78.2%; mp 271−272 °C; ^{1}H NMR (600 MHz, DMSO-d_6) δ 11.45 (s, 1H), 8.51−8.44 (m, 1H), 8.06−8.01 (m, 1H), 7.99 (d, J = 2.5 Hz, 1H), 7.89−7.85 (m, 2H), 7.74 (dd, J = 8.7, 2.5 Hz, 1H), 7.54 (d, J = 8.7 Hz, 1H)

General Procedures for the Preparation of Intermediates 76−78. 6-(3-Bromopropoxy)-2-(3,4-dichlorophenyl)-4,5-dimethylpyridazin-3(2*H*)-one (76). To a solution of **73** (10 mmol) and 1,3-dibromopropane (20 mmol) in acetone (100 mL), potassium carbonate (20 mmol) was added, and the mixture was refluxed for 4−6 h. The progress of the reaction was monitored by TLC. After cooling to room temperature, the mixture was filtered and the solvent was evaporated under reduced pressure. The crude product was purified by means of chromatography (petroleum ether/EtOAc = 15/1) to yield compound **76**. Pale yellow oil; yield 71.8%; ^{1}H NMR (600 MHz, $CDCl_3$) δ 7.93 (dd, J = 2.3, 1.0 Hz, 1H), 7.67 (ddd, J = 8.7, 2.4, 1.0 Hz, 1H), 7.51 (dd, J = 8.7, 0.9 Hz, 1H), 4.40−4.27 (m, 2H), 3.59 (td, J = 6.4, 0.7 Hz, 2H), 2.36 (p, J = 5.8 Hz, 2H), 2.23 (s, 3H), 2.17 (s, 3H).

4-(3-Bromopropoxy)-2-(3,4-dichlorophenyl)-5,6,7,8-tetrahydrophthalazin-1(2*H*)-one (77). Pale yellow solid; yield 72.4%; mp 45−46 °C; ^{1}H NMR (600 MHz, $CDCl_3$) δ 7.93 (d, J = 2.5 Hz, 1H), 7.68 (dd, J = 8.7, 2.5 Hz, 1H), 7.50 (d, J = 8.7 Hz, 1H), 4.33 (t, J = 5.9 Hz, 2H), 3.58 (t, J = 6.5 Hz, 2H), 2.61 (t, J = 4.7 Hz, 2H), 2.53 (dd, J = 5.4, 3.9 Hz, 2H), 2.34 (p, J = 6.2 Hz, 2H), 1.89−1.74 (m, 4H).

4-(3-Bromopropoxy)-2-(3,4-dichlorophenyl)phthalazin-1(2*H*)-one (78). Pale yellow solid; yield 72.4%; mp 48−50 °C; ^{1}H NMR (600 MHz, $CDCl_3$) δ 8.51−8.44 (m, 1H), 8.06−8.01 (m, 1H), 7.99 (d, J = 2.5 Hz, 1H), 7.89−7.85 (m, 2H), 7.74 (dd, J = 8.7, 2.5 Hz, 1H), 7.54 (d, J = 8.7 Hz, 1H), 4.54 (t, J = 5.9 Hz, 2H), 3.66 (t, J = 6.5 Hz, 2H), 2.46 (p, J = 6.2 Hz, 2H).

General Procedures for the Synthesis of Compounds 79−81. Method B. 2-(3,4-Dichlorophenyl)-4,5-dimethyl-6-(3-(piperidin-1-yl)propoxy)pyridazin-3(2*H*)-one (79). To a suspension of **73** (2 mmol) and piperidine (2.2 mmol), K_2CO_3 (4 mmol) in acetonitrile (50 mL) and a catalytic amount of KI (1% mol) were added, and the resulting mixture was refluxed for 6−8 h. After filtering, the resulting filtrate was evaporated to dryness under reduced pressure. The residue was suspended in water (10.0 mL) and extracted with dichloromethane (3 × 25 mL). The combined organic layers were dried with anhydrous magnesium sulfate, the filtrate was evaporated under reduced pressure, and the crude product was purified by means of chromatography (10% MeOH/$CHCl_3$) to yield compounds **79**. Pale yellow oil; yield 82.1%; ^{1}H NMR (600 MHz, $CDCl_3$) δ 7.92 (d, J = 2.5 Hz, 1H), 7.76−7.64 (m, 1H), 7.49 (dd, J = 7.7, 3.4 Hz, 1H), 4.21 (t, J = 6.3 Hz, 2H), 2.50−2.43 (m, 6H), 2.24−2.21 (m, 3H), 2.20−2.13 (m, 3H), 2.04−1.94 (m, 2H), 1.68−1.58 (m, 4H), 1.46 (br, 2H). HRMS (ESI) m/z 410.1405 (calcd 410.1397 for $C_{20}H_{26}Cl_2N_3O_2$ $[M + H]^+$).

2-(3,4-Dichlorophenyl)-4-(3-(piperidin-1-yl)propoxy)-5,6,7,8-tetrahydrophthalazin-1(2*H*)-one (80). Pale yellow oil; yield 79.8%; ^{1}H NMR (600 MHz, $CDCl_3$) δ 7.92 (d, J = 2.5 Hz, 1H), 7.67 (dd, J = 8.7, 2.5 Hz, 1H), 7.48 (d, J = 8.7 Hz, 1H), 4.21 (t, J = 6.3 Hz, 2H), 2.64−2.29 (m, 10H), 2.05−1.92 (m, 2H), 1.83−1.71 (m, 4H), 1.66−1.53 (m, 4H), 1.46 (br, 2H). HRMS (ESI) m/z 463.1557 (calcd 436.1553 for $C_{22}H_{28}Cl_2N_3O_2$ $[M + H]^+$).

2-(3,4-Dichlorophenyl)-4-(3-(piperidin-1-yl)propoxy)-phthalazin-1(2*H*)-one (81). Pale yellow oil; yield 80.3%; ^{1}H NMR (600 MHz, $CDCl_3$) δ 8.49−8.43 (m, 1H), 8.06−8.00 (m, 1H), 7.98 (d, J = 2.5 Hz, 1H), 7.86−7.73 (m, 2H), 7.74 (dd, J = 8.7, 2.5 Hz, 1H), 7.52 (d, J = 8.7 Hz, 1H), 4.41 (t, J = 6.3 Hz, 2H), 2.58−2.47 (m, 6H), 2.20−2.06 (m, 2H), 1.66−1.57 (m, 4H), 1.47 (br, 2H). HRMS (ESI) m/z 432.1249 (calcd 432.1240 for $C_{22}H_{24}Cl_2N_3O_2$ $[M + H]^+$).

Single Crystal X-ray Structure Determination of 54. Crystallization and Sample Preparation. Crystals of the hydrochloride salt of **54** were obtained by slow evaporation of cosolvent of methanol and acetone solution of the compound.

Data Collection. Crystal structure determination for the hydrochloride salt of **54** was carried out using Bruker SMART APEX II.

Structure Solution and Refinement. Crystal structure solution was achieved using direct methods as implemented in SHELXTL[66] and visualized using the program XP. Missing atoms were subsequently located from difference Fourier synthesis and added to the atom list. Least-squares refinement on F^2 using all measured intensities was carried out using the program SHELXTL. All non-hydrogen atoms were refined, including anisotropic displacement parameters. The chlorine anion corresponding to one cationic molecule is distributed in two half-positions located on 2-fold rotation axes and shared with the neighboring cationic molecules.

Crystal Data at sf20150715_zyc_0m. $C_{18}H_{26}Cl_3N_3O_4$, crystal size 0.39 × 0.32 × 0.3 mm^3, 454.77 g mol^{-1}, triclinic, $P1$, a = 8.7813(3) Å, b = 10.4026(3) Å, c = 12.2094(4) Å, α = 97.6772(14)°, β = 91.8626(13)°, γ = 105.0210(12)°, V = 1064.92(6) Å^3, Z = 2, ρ_{calcd} =1.418 Mg/m^3, R1 = 0.0364 (0.0427), wR2 = 0.1002 (0.1063), absorption coefficient is 0.459 mm^{-1}, $F(000)$ = 476, goodness-of-fit on F^2 is 1.028, largest difference peak (hole) is 0.337 (−0.289) e Å^{-3}.

DOI: 10.1021/acs.jmedchem.5b01416
J. Med. Chem. XXXX, XXX, XXX−XXX

Receptor Binding Studies. Materials. The following specific radioligands and tissue sources were used: (a) σ_1 receptor, [^{3}H]-(+)-pentazocine (250 μCi, PerkinElmer, NET-1056250UC), and male Dunkin Hartley guinea pig brain membrane; (b) σ_2 receptor, [^{3}H]-di-*o*-tolylguanidine ([^{3}H]-DTG, 250 μCi, PerkinElmer, NET-986250UC), (+)-SKF-10047 (Sigma-Aldrich), and male Dunkin Hartley guinea pig brain membrane. Chemicals and reagents were purchased from different commercial sources and of analytical grade.

Membrane Preparation. Membrane preparation was performed by previously reported method.[36] Crude P2 membranes were prepared from frozen guinea pig brains minus cerebellum. Tissues were homogenized in ice-cold 10 mmol Tris-sucrose buffer (0.32 mol sucrose in 10 mmol Tris-HCl, pH 7.4) using an ULTRA TURAX homogenizer. The homogenates were centrifuged at 4 °C at 1000*g* for 10 min, and the supernatant was saved. The resulting pellet was then resuspended in the same buffer, incubated for 10 min at 4 °C, and centrifuged at 1000*g* for 10 min. After that, the pellet was discarded and the supernatants were combined and centrifuged at 31 000*g* for 15 min. The pellets were resuspended in 10 mL of Tris-HCl, pH 7.4, in a volume of 3 mL/g, and the suspension was allowed to incubate at 25 °C for 30 min. Following centrifuging at 31 000*g* for 15 min, the pellet was resuspended by gentle homogenization in 10 mmol of Tris-HCl, pH 7.4, in a final volume of 1.53 mL/g tissue and aliquots were stored at −80 °C until used. The protein concentration of the suspension was determined by the method of Bradford.[67] Subsequently, the preparation contained 4 mg protein/mL.

General Procedures for the Binding Assays. All the test compounds were prepared by dissolving in 5% DMSO. The filter mats were presoaked in 0.5% polyethylenimine solution for 2 h at room temperature before use. The following specific radioligands and tissue sources were used: (a) σ_1 receptor, [^{3}H]-(+)-pentazocine, guinea pig brain membranes; (b) σ_2 receptor, [^{3}H]-DTG, (+)-SKF-10047 (blocked the σ_1 receptor) guinea pig brain membranes.

For the σ_1 receptor binding assays, the total binding (TB) was determined in the presence of the radioligand [^{3}H]-(+)-pentazocine. Nonspecific binding (NB) was determined in the presence of the radioligand [^{3}H]-(+)-pentazocine and haloperidol, while the compound binding (CB) was determined in the presence of the radioligand [^{3}H]-(+)-pentazocine and the determining compound. Specific binding (SB) is calculated by the total binding (TB) minus the nonspecific binding (NB) at a particular concentration of radioligand. Percentage of inhibition (%) was calculated as the following equation: percentage of inhibition (%) = $[(TB - CB)/(TB - NB)] \times 100$.

Blank experiments were carried out to determine the effect of 5% DMSO on the binding, and no effects were observed. Compounds were tested at least three times over a 6 concentration range (10^{-5} mol to 10^{-10} mol), and IC_{50} values were determined by nonlinear regression analysis using Hill equation curve fitting. K_i values were calculated based on the Cheng and Prusoff equation: $K_i = IC_{50}/(1 + C/K_d)$. In the equation, C represents the concentration of the hot ligand used, and K_d, its receptor dissociation constant, was calculated for each labeled ligand (for [^{3}H]-(+)-pentazocine, K_d was 1.53 ± 0.30 nM (n = 3), and for [^{3}H]-DTG, K_d was 6.76 ± 0.94 nM (n = 3)). Mean K_i values and SEM are reported for at least three independent experiments.

σ_1 Receptor Binding Assays. Binding of [^{3}H]-(+)-pentazocine at σ_1 receptor was performed according to D. L. Dehaven-Hudkins et al.[54] with minor modifications.[42,43] The binding properties of the test compounds to guinea pig σ_1 receptor were studied in guinea pig brain membranes using [^{3}H]-(+)-pentazocine as the radioligand. To each total binding assay tube were added 900 μL of the tissue suspension, 50 μL of 4.0 nM [^{3}H]-(+)-pentazocine, 50 μL Tris-HCl buffer, pH 8.0. To nonspecific binding each assay tube were added 900 μL of the tissue suspension, 50 μL of [^{3}H]-(+)-pentazocine, 50 μL of 10 μM haloperidol. To each specific binding assay tube were added 900 μL of the tissue suspension, 50 μL of [^{3}H]-(+)-pentazocine, 50 μL of reference drug or test compounds solution in various concentrations (10^{-5} mol to 10^{-10} mol). The tubes were incubated at 25 °C for 180 min. The incubation was followed by a rapid vacuum filtration through Whatman GF/B glass filters, and the filtrates were washed twice with 5 mL of cold buffer and transferred to scintillation vials. Scintillation fluid (2.0 mL) was added, and the radioactivity bound was measured using a Beckman LS 6500 liquid scintillation counter.

σ_2 Receptor Binding Assays. Binding assays were performed as described by Ronsisvalle et al.[36] with minor modifications.[68] The binding properties of the test compounds to guinea pig σ_2 receptor were studied in guinea pig brain membranes using [^{3}H]-DTG. The membranes were incubated with 3 nM [^{3}H]-DTG in the presence of 400 nM (+)-SKF-10047 to block σ_1 sites. To each total binding assay tube were added 850 μL of the tissue suspension, 50 μL of 3.0 nM [^{3}H]-DTG, 50 μL of 400 nM (+)-SKF-10047, 50 μL Tris-HCl buffer, pH 8.0. To each nonspecific binding assay tube were added 850 μL of the tissue suspension, 50 μL of [^{3}H]-DTG, 50 μL of 400 nM (+)-SKF-10047, 50 μL of 10 μM DTG. To each specific binding assay tube were added 850 μL of the tissue suspension, 50 μL of [^{3}H]-DTG, 50 μL of 400 nM (+)-SKF-10047, 50 μL of reference drug or test compounds solution in various concentrations (10^{-5} mol to 10^{-10} mol). The tubes were incubated at 25 °C for 120 min. The incubation was followed by a rapid vacuum filtration through Whatman GF/B glass filters, and the filtrates were washed twice with 5 mL of cold buffer and transferred to scintillation vials. Scintillation fluid (2.0 mL) was added, and the radioactivity bound was measured using a Beckman LS 6500 liquid scintillation counter.

Functional Profile on σ_1 Receptor. The functional activity of compound **54** was evaluated by using guinea pig brain membranes binding assays for σ_1 receptor. The binding affinities in either the absence or presence of 1 mM phenytoin were measured to identify the functional (agonistic or antagonistic) nature.[59]

In Vivo Test. Animals. Chinese Kun Ming (KM) mice (20 ± 2.0 g) and Sprague−Dawley (SD) rats (250 ± 5.0 g) were used as experimental animals in this study. All the animals were housed under standardized conditions for light, temperature, and humidity and received standard rat chow and tap water and libitum. Animals were assigned to different experimental groups randomly, each kept in a separate cage. All studies involving animals in this research follow the guidelines of the bylaw of experiments on animals and have been approved by the Ethics and Experimental Animal Committee of Jiangsu Nhwa Pharmaceutical Co., Ltd.

Acute Toxicity. Mice (10 mice for each group) were orally dosed with po administration of a 10 mL/kg volume of vehicle 0.5% methylcellulose (Sigma-Aldrich) or increasing dose of test compounds (200, 500, 1000, 1500, and 2000 mg/kg). The number of surviving animals was recorded after 24 h of drug administration. The percent mortality in each group was calculated. The LD_{50} values were calculated by using Statistical Package for Social Sciences (SPSS) program.

hERG Affinity. Ability to block hERG potassium channels was determined using the whole-cell patch clamp method and cloned hERG potassium channels (expressed in HEK 293 cells) as biological material.[55] For this purpose, the patch clamp amplifier (Axopatch 200B, Molecular Devices) and digital converter (Digidata 1440A, Molecular Devices) were used. Recording electrodes were made from borosilicate glass with filament (BF120-94-15, Sutter Instrument Company). Creation of voltage-clamp command pulse protocols and data acquisition were controlled by pCLAMP software (version 10.1, Molecular Devices).

The bath solution consisted of 137 mM NaCl, 5.4 mM KCl, 10 mM glucose, 10 mM HEPES, and 2 mM $CaCl_2$. The pH was adjusted to 7.5 by addition of NaOH. The pipet filling solution consisted of 140 mM KCl, 1 mM $MgCl_2$, 5 mM EGTA, 10 mM HEPES, and 5 mM Na_2ATP. The pH was adjusted to 7.2 by addition of KOH.

To study voltage dependence of steady-state block of hERG channels on different drug concentrations (0.3, 1, 3, and 10 μM) in HEK cells, the holding membrane potential was switched from −80 to +50 mV for 2 s following return to −50 mV for 3 s (sampling rate of 4 kHz, low-pass filtered at 1 kHz) in intervals of 30 s. Tail currents were measured at −50 mV in control and in the presence of the drug at concentrations determined empirically. All raw measurements were performed using Clampfit (version 10.2), a part of pCLAMP software (version 10.1). Results were transferred to the program Statistical

DOI: 10.1021/acs.jmedchem.5b01416
J. Med. Chem. XXXX, XXX, XXX−XXX

Package for the Social Sciences (SPSS) spreadsheets for further analysis.

Formalin Test. Formalin tests were performed as described by Cendán et al.[61] with minor modifications. A diluted formalin solution (20 μL of a 2.5% formalin solution, 0.92% formaldehyde) was injected into the dorsal surface of the right hind paw of the mouse. Immediately thereafter, the mouse was put into a glass cylinder and the observation period started. A mirror was placed behind the glass cylinder to allow clear observation of the paws. Nociceptive behavior induced by formalin was quantified as the time spent licking or biting the injected paw during two different periods individually recorded: the first period was recorded 0−5 min after the injection of formalin and was considered indicative of formalin-evoked nociception phase I; the second period was recorded 15−45 min after formalin injection and was considered indicative of formalin-voked nociception phase II.[49] The mice (n = 10−12 per group) received ip administration of a 10 mL/kg volume of vehicle 30% PEG 400 (Sigma-Aldrich) or test compound 15 min before intraplantar (ipl) formalin injection.

The antinociceptive effect induced by the different treatments in the formalin test was calculated by the following formula: antinociceptive effect (%) = $[(LT_V - LT_D)/LT_V] \times 100$, where LT_V represent the licking time in vehicle injected animals, LT_D means licking time in drug-injected animals.

CCI Model.[62,63] The CCI of the sciatic nerve as an animal model was used to study the efficacy of treatments in neuropathic pain. Rats were randomly separated into several groups: sham control and vehicle- and drug-treated groups, and each group contained 10 rats. Pain threshold base values of each group were measured 1−2 days before surgery, and those with the value of 2 days were picked. The pain thresholds were measured again 14 days after surgery to check whether the model was successful. Drugs were dose orally with po administration of a 10 mL/kg volume of vehicle 0.5% methylcellulose (Sigma-Aldrich) or increasing dose of test compounds twice a day for 4 days (15th, 16th, 17th, and 18th day). Each group was measured after first administration on the 15th day and the last administration on the 18th day, which resulted in the single administration and repeated administration, respectively.

The CCI of the sciatic nerve surgery was performed as described by Bennett and Xie[62a] with minor modification. Briefly, the SD rats were anesthetized with chloral hydrate (5%) and the right common sciatic nerve was exposed at the level of the midthigh of the right hind paw. At about 1 cm proximal to the nerve trifurcation, about 7 mm of the nerve was freed and four ligatures (4−0 silk tread) were tight loosely with a distance of ∼1.0 mm. The nerve was only barely constricted. The muscle was than stitched and the skin incision closed with wound clips. The rats with sciatic nerve exposure without ligation served as the sham control group. Two tests were performed: the von Frey test (electronic von Frey rigid tips with 90 g range (IITC Life Science Inc., U.S.A, 2390)) and the plantar test. Allodynia to mechanical stimuli and hyperalgesia to noxious thermal stimulus were used as outcome measures of neuropathic pain by using the von Frey and plantar tests, respectively. In the von Frey test, briefly, animals were placed in a transparent test chamber with a wire-mesh grid floor through which von Frey monofilaments were applied. The monofilaments were applied in increasing force until the rats withdrew the ipsilateral, nerve injury paw using an up−down paradigm. Clear paw withdrawal, sharking, or licking was considered as nociceptive-lick response to determine the mechanical withdrawal threshold (MWT). Animals were adapted to the testing situation for at least 30 min before the sessions started. For each measurement, the paw was sampled four times and a mean calculated. At least 3 min elapsed between. Thermal hyperalgesia was assessed through the plantar test by measuring hind paw latency in response to radiant heat. Briefly, rats were placed in a clear plastic chamber with a glass floor and allowed to acclimate to the environment for 30 min. A radiant heat source (BMC-410A) was then positioned under the plantar surface of the hind paw. The latency for the withdrawal reflex was recorded as thermal withdrawal latency (TWL). A cutoff time of 30 s was imposed to prevent tissue damage in the absence of response. For each measurement, the paw was sampled four times and a mean calculated. At least 3 min elapsed between.

Motor Coordination (Rotarod Test).[42] The motor performance of mice was assessed by means of an automated rotarod (YLS-4C, China). Mice were trained, and those that could not stay moving on the rod for 300 s in 10 rpm were discarded from the study before drug treatment. In the test, mice were required to walk against the motion of an elevated rotating drum at 10 rpm and the latencies to fall-down were recorded. With the selected animals, rotarod latencies were measured 30, 60, 90, and 120 min after ig administration of drugs.

Locomotor Activity Test. Locomotor activity was assessed in 14 automated activity frames equipped with infrared photobeam emitters and sensors. To assess drug effect on exploratory locomotor activity, the mice were transferred to new home cages immediately before test start and activity was measured for 30 min. Test or reference compounds were orally administered 30 min before test start at the following doses of 40, 80, 160 mg/kg; haloperidol was at 0.1, 0.3, 1 mg/kg. The average speed was measured before and 30, 60, 90, and 120 min after treatment.

Pharmacokinetics Study in Rats. The HPLC conditions were as follows: column, XSELECT CSH XP C18 (2.1 mm × 50 mm, 2.5 μm); mobile phase, 0.025% FA and 1 mM NH_4OAc (ROE SCIENTIFIC INC, USA) in water/acetonitrile (Merck Company, Germany) (v:v, 45:55); flow rate, 0.6 mL/min; column temperature, 50 °C. UV detection was performed at 210 nm. For routine compound **54** screening, rats (n = 3/group) were dosed via the lateral tail vein at the indicated dose for iv administration (5 mg/kg, 100% saline) or via oral gavage (80 mg/kg, suspension in 0.5% methylcellulose). At 30 min and 1, 2, 3, 4, 5, 6, 8 and 24 h after administration, serial blood samples were collected from the lateral tail vein into heparinized collection tubes (approximately 0.25 mL). The plasma was separated by centrifugation, and the sample was prepared for LC/MS analysis by protein precipitation with acetonitrile. The plasma samples were analyzed for drug and internal standard via the LC−MS/MS protocol.

Statistics. To estimate the potency of test and reference compounds, the ED_{50} values and their 95% confidence limits were calculated by using the program SPSS (Statistical Package for the Social Science).

■ ASSOCIATED CONTENT

Supporting Information

The Supporting Information is available free of charge on the ACS Publications website at DOI: 10.1021/acs.jmedchem.5b01416. CCDC 1423214 contains the supplementary crystallographic data for this paper. These data can be obtained free of charge via www.ccdc.cam.ac.uk/conts/retrieving.html (or from the Cambridge Crystallographic Data Centre, 12 Union Road, Cambridge CB21EZ, U.K. (fax (+44) 1223-336-033, e-mail deposit@ccdc.cam.ac.uk).

Inhibition curves of functional profile of σ_1 receptor; additional receptors binding affinities of compound **54**; data of compound 54 in phase I of the mouse formalin test; ^{1}H NMR, HR-MS, and HPLC of compound **54**; X-ray crystal data of compound **54** (PDF)

Molecular formula strings (CSV)

■ AUTHOR INFORMATION

Corresponding Author

*E-mail: gszhang@mail.hust.edu.cn. Phone: +86-27-87792235. Fax: +86-27-87792170.

Author Contributions

§X.C. and Y.C. contributed equally to this work.

Notes

The authors declare no competing financial interest.

DOI: 10.1021/acs.jmedchem.5b01416
J. Med. Chem. XXXX, XXX, XXX−XXX

■ ACKNOWLEDGMENTS

We are grateful for financial support from the NSFC (Grant 81573291) and the National Science and Technology Major Project "Key New Drug Creation and Manufacturing Program" (Grant 2012ZX09103-101-010). The authors thank Prof. Liangren Zhang, Zhenming Liu, and Hongwei Jin of State Key Laboratory of Natural and Biomimetic Drugs, School of Pharmaceutical Sciences, Peking University, for performing HRMS.

■ ABBREVIATIONS USED

CNS, central nervous system; NMDA, *N*-methyl-D-aspartate; hERG, ether-a-go-go-related gene; ig, intragastric administration; CCI, chronic constriction injury; ED_{50}, 50% effective dose; LD_{50}, median lethal dose

■ REFERENCES

(1) Jongen, J. L.; Hans, G.; Benzon, H. T.; Huygen, F.; Hartrick, C. T. Neuropathic pain and pharmacological treatment. *Pain. Pract.* **2014**, *14*, 283−295.
(2) van Hecke, O.; Austin, S. K.; Khan, R. A.; Smith, B. H.; Torrance, N. Neuropathic pain in the general population: a systematic review of epidemiological studies. *Pain* **2014**, *155*, 654−662.
(3) Gilron, I.; Dickenson, A. H. Emerging drugs for neuropathic pain. *Expert Opin. Emerging Drugs* **2014**, *19*, 329−341.
(4) Turk, D. C.; Wilson, H. D.; Cahana, A. Treatment of chronic non-cancer pain. *Lancet* **2011**, *377*, 2226−2235.
(5) (a) Kissin, I. The development of new analgesics over the past 50 years: a lack of real breakthrough drugs. *Anesth. Analg.* **2010**, *110*, 780−789. (b) Burgess, G.; Williams, D. The discovery and development of analgesics: new mechanisms, new modalities. *J. Clin. Invest.* **2010**, *120*, 3753−3759.
(6) (a) Vela, J. M.; Merlos, M.; Almansa, C. Investigational sigma-1 receptor antagonists for the treatment of pain. *Expert Opin. Invest. Drugs* **2015**, *24*, 883−896. (b) Davis, M. P. Sigma-1 receptors and animal studies centered on pain and analgesia. *Expert Opin. Drug Discovery* **2015**, *10*, 885−900.
(7) Dworkin, R. H.; O'Connor, A. B.; Backonja, M.; Farrar, J. T.; Finnerup, N. B.; Jensen, T. S.; Kalso, E. A.; Loeser, J. D.; Miaskowski, C.; Nurmikko, T. J.; Portenoy, R. K.; Rice, A. S.; Stacey, B. R.; Treede, R. D.; Turk, D. C.; Wallace, M. S. Pharmacologic management of neuropathic pain: evidence-based recommendations. *Pain* **2007**, *132*, 237−251.
(8) Attal, N.; Cruccu, G.; Baron, R.; Haanpää, M.; Hansson, P.; Jensen, T. S.; Nurmikko, T.; European Federation of Neurological Societies.. EFNS guidelines on the pharmacological treatment of neuropathic pain: 2010 revision. *Eur. J. Neurol.* **2010**, *17*, 1113−1123.
(9) Moulin, D.; Boulanger, A.; Clark, A. J.; Clarke, H.; Dao, T.; Finley, G. A.; Furlan, A.; Gilron, I.; Gordon, A.; Morley-Forster, P. K.; Sessle, B. J.; Squire, P.; Stinson, J.; Taenzer, P.; Velly, A.; Ware, M. A.; Weinberg, E. L.; Williamson, O. D. Pharmacological management of chronic neuropathic pain: revised consensus statement from the Canadian Pain Society. *Pain. Res. Manag.* **2014**, *19*, 328−335.
(10) Cohen, S. P.; Mao, J. Neuropathic pain: mechanisms and their clinical implications. *BMJ.* **2014**, *348*, f7656.
(11) Dworkin, R. H.; O'Connor, A. B.; Audette, J.; Baron, R.; Gourlay, G. K.; Haanpää, M. L.; Kent, J. L.; Krane, E. J.; Lebel, A. A.; Levy, R. M.; Mackey, S. C.; Mayer, J.; Miaskowski, C.; Raja, S. N.; Rice, A. S.; Schmader, K. E.; Stacey, B.; Stanos, S.; Treede, R. D.; Turk, D. C.; Walco, G. A.; Wells, C. D. Recommendations for the pharmacological management of neuropathic pain: an overview and literature update. *Mayo Clin. Proc.* **2010**, *85*, s3−s14.
(12) Zukin, S. R.; Brady, K. T.; Slifer, B. L.; Balster, R. L. Behavioral and biochemical stereoselectivity of sigma opiate/PCP receptors. *Brain Res.* **1984**, *294*, 174−177.
(13) Mendelsohn, L. G.; Kalra, V.; Johnson, B. G.; Kerchner, G. A. Sigma opioid receptor: characterization and co-identity with the phencyclidine receptor. *J. Pharmacol. Exp. Ther.* **1985**, *233*, 597−602.
(14) Hellewell, S. B.; Bowen, W. D. A sigma-like binding site in rat pheochromocytoma (PC12) cells: decreased affinity for (+)-benzomorphans and lower molecular weight suggest a different sigma receptor form from that of guinea pig brain. *Brain Res.* **1990**, *527*, 244−253.
(15) Quirion, R.; Bowen, W. D.; Itzhak, Y.; Junien, J. L.; Musacchio, J. M.; Rothman, R. B.; Su, T. P.; Tam, S. W.; Taylor, D. P. A proposal for the classification of sigma binding sites. *Trends Pharmacol. Sci.* **1992**, *13*, 85−86.
(16) Maurice, T.; Su, T. P. The pharmacology of sigma-1 receptors. *Pharmacol. Ther.* **2009**, *124*, 195−206.
(17) Zamanillo, D.; Romero, L.; Merlos, M.; Vela, J. M. Sigma 1 receptor: a new therapeutic target for pain. *Eur. J. Pharmacol.* **2013**, *716*, 78−93.
(18) Monnet, F. P.; Debonnel, G.; Junien, J. L.; De Montigny, C. N-methyl-D-aspartate-induced neuronal activation is selectively modulated by sigma receptors. *Eur. J. Pharmacol.* **1990**, *179*, 441−445.
(19) Cheng, Z. X.; Lan, D. M.; Wu, P. Y.; Zhu, Y. H.; Dong, Y.; Ma, L.; Zheng, P. Neurosteroid dehydroepiandrosterone sulphate inhibits persistent sodium currents in rat medial prefrontal cortex via activation of sigma-1 receptors. *Exp. Neurol.* **2008**, *210*, 128−136.
(20) Aydar, E.; Palmer, C. P.; Klyachko, V. A.; Jackson, M. B. The sigma receptor as a ligand-regulated auxiliary potassium channel subunit. *Neuron* **2002**, *34*, 399−410.
(21) Hayashi, T.; Maurice, T.; Su, T. P. Ca^{2+} signaling via sigma(1)-receptors: novel regulatory mechanism affecting intracellular Ca^{2+} concentration. *J. Pharmacol. Exp. Ther.* **2000**, *293*, 788−798.
(22) Sánchez-Fernández, C.; Montilla-García, Á.; González-Cano, R.; Nieto, F. R.; Romero, L.; Artacho-Cordón, A.; Montes, R.; Fernández-Pastor, B.; Merlos, M.; Baeyens, J. M.; Entrena, J. M.; Cobos, E. J. Modulation of peripheral mu-opioid analgesia by σ_1 receptors. *J. Pharmacol. Exp. Ther.* **2014**, *348*, 32−45.
(23) Roh, D. H.; Kim, H. W.; Yoon, S. Y.; Seo, H. S.; Kwon, Y. B.; Kim, K. W.; Han, H. J.; Beitz, A. J.; Na, H. S.; Lee, J. H. Intrathecal injection of the σ_1 receptor antagonist BD1047 blocks both mechanical allodynia and increases in spinal NR1 expression during the induction phase of rodent neuropathic pain. *Anesthesiology* **2008**, *109*, 879−889.
(24) (a) Banister, S. D.; Manoli, M.; Kassiou, M. The development of radiotracers for imaging sigma (σ) receptors in the central nervous system (CNS) using positron emission tomography (PET). *J. Labelled Compd. Radiopharm.* **2013**, *56*, 215−224. (b) van Waarde, A.; Rybczynska, A. A.; Ramakrishnan, N.; Ishiwata, K.; Elsinga, P. H.; Dierckx, R. A. Sigma receptors in oncology: therapeutic and diagnostic applications of sigma ligands. *Curr. Pharm. Des.* **2010**, *16*, 3519−3537.
(25) Crawford, K. W.; Bowen, W. D. Sigma-2 receptor agonists activate a novel apoptotic pathway and potentiate antineoplastic drugs in breast tumor cell lines. *Cancer Res.* **2002**, *62*, 313−322.
(26) Mach, R. H.; Zeng, C.; Hawkins, W. G. The sigma-2 receptor: a novel protein for the imaging and treatment of cancer. *J. Med. Chem.* **2013**, *56*, 7137−7160.
(27) Nguyen, L.; Lucke-Wold, B. P.; Mookerjee, S. A.; Cavendish, J. Z.; Robson, M. J.; Scandinaro, A. L.; Matsumoto, R. R. Role of sigma-1 receptors in neurodegenerative diseases. *J. Pharmacol. Sci.* **2015**, *127*, 17−29.
(28) Robson, M. J.; Turner, R. C.; Naser, Z. J.; McCurdy, C. R.; O'Callaghan, J. P.; Huber, J. D.; Matsumoto, R. R. SN79, a sigma receptor antagonist, attenuates methamphetamine-induced astrogliosis through a blockade of OSMR/gp130 signaling and STAT3 phosphorylation. *Exp. Neurol.* **2014**, *254*, 180−189.
(29) (a) Hiranita, T.; Mereu, M.; Soto, P. L.; Tanda, G.; Katz, J. L. Self-administration of cocaine induces dopamine-independent self-administration of sigma agonists. *Neuropsychopharmacology* **2013**, *38*, 605−615. (b) Cao, J.; Kopajtic, T.; Katz, J. L.; Newman, A. H. Dual DAT/σ_1 receptor ligands based on 3-(4-(3-(bis(4-fluorophenyl)-amino)propyl)piperazin-1-yl)-1-phenylpropan-1-ol. *Bioorg. Med. Chem. Lett.* **2008**, *18*, 5238−5241. (c) Hiranita, T.; Mereu, M.; Soto,

DOI: 10.1021/acs.jmedchem.5b01416
J. Med. Chem. XXXX, XXX, XXX−XXX

P. L.; Tanda, G.; Katz, J. L. Self-administration of cocaine induces dopamine-independent self-administration of sigma agonists. *Neuropsychopharmacology* **2013**, *38*, 605−615.
(30) (a) James, M. L.; Shen, B.; Zavaleta, C. L.; Nielsen, C. H.; Mesangeau, C.; Vuppala, P. K.; Chan, C.; Avery, B. A.; Fishback, J. A.; Matsumoto, R. R.; Gambhir, S. S.; McCurdy, C. R.; Chin, F. T. New positron emission tomography (PET) radioligand for imaging sigma-1 receptors in living subjects. *J. Med. Chem.* **2012**, *55*, 8272−8282. (b) Poupaert, J.; Carato, P.; Colacino, E.; Yous, S. 2(3H)-benzoxazolone and bioisosters as "privileged scaffold" in the design of pharmacological probes. *Curr. Med. Chem.* **2005**, *12*, 877−885. (c) Yous, S.; Wallez, V.; Belloir, M.; Caignard, D. H.; McCurdy, C. R.; Poupaert, J. H. Novel 2(3H)-benzothiazolones as highly potent and selective sigma-1 receptor ligands. *Med. Chem. Res.* **2005**, *14*, 158−168.
(31) Tsai, S. Y.; Pokrass, M. J.; Klauer, N. R.; De Credico, N. E.; Su, T. P. Sigma-1 receptor chaperones in neurodegenerative and psychiatric disorders. *Expert Opin. Ther. Targets* **2014**, *18*, 1461−1476.
(32) Bermack, J. E.; Debonnel, G. The role of sigma receptors in depression. *J. Pharmacol. Sci.* **2005**, *97*, 317−336.
(33) Ovalle, S.; Andreu, F.; Pérez, M. P.; Zamanillo, D.; Guitart, X. Effect of the novel σ_1 receptor ligand and putative atypical antipsychotic E-5842 on BDNF mRNA expression in the rat brain. *NeuroReport* **2002**, *13*, 2345−2348.
(34) Hayashi, T.; Su, T. P. The potential role of sigma-1 receptors in lipid transport and lipid raft reconstitution in the brain: implication for drug abuse. *Life Sci.* **2005**, *77*, 1612−1624.
(35) Meunier, J.; Gué, M.; Récasens, M.; Maurice, T. Attenuation by a sigma-1 (σ_1) receptor agonist of the learning and memory deficits induced by a prenatal restraint stress in juvenile rats. *Br. J. Pharmacol.* **2004**, *142*, 689−700.
(36) Ronsisvalle, G.; Marrazzo, A.; Prezzavento, O.; Cagnotto, A.; Mennini, T.; Parenti, C.; Scoto, G. M. Opioid and sigma receptor studies. New developments in the design of selective sigma ligands. *Pure Appl. Chem.* **2001**, *73*, 1499−1509.
(37) de Costa, B. R.; Radesca, L.; Di Paolo, L.; Bowen, W. D. Synthesis, characterization, and biological evaluation of a novel class of N-(arylethyl)-N-alkyl-2-(1-pyrrolidinyl)ethylamines: structural requirements and binding affinity at the sigma receptor. *J. Med. Chem.* **1992**, *35*, 38−47.
(38) Entrena, J. M.; Cobos, E. J.; Nieto, F. R.; Cendán, C. M.; Gris, G.; Del Pozo, E.; Zamanillo, D.; Baeyens, J. M. Sigma-1 receptors are essential for capsaicin-induced mechanical hypersensitivity: studies with selective sigma-1 ligands and sigma-1 knockout mice. *Pain* **2009**, *143*, 252−261.
(39) Díaz, J. L.; Cuberes, R.; Berrocal, J.; Contijoch, M.; Christmann, U.; Fernández, A.; Port, A.; Holenz, J.; Buschmann, H.; Laggner, C.; Serafini, M. T.; Burgueño, J.; Zamanillo, D.; Merlos, M.; Vela, J. M.; Almansa, C. Synthesis and biological evaluation of the 1-arylpyrazole class of σ_1 receptor antagonists: identification of 4-{2-[5-methyl-1-(naphthalen-2-yl)-1H-pyrazol-3-yloxy]ethyl}morpholine (S1RA, E-52862). *J. Med. Chem.* **2012**, *55*, 8211−8224.
(40) Romero, L.; Zamanillo, D.; Nadal, X.; Sánchez-Arroyos, R.; Rivera-Arconada, I.; Dordal, A.; Montero, A.; Muro, A.; Bura, A.; Segalés, C.; Laloya, M.; Hernández, E.; Portillo-Salido, E.; Escriche, M.; Codony, X.; Encina, G.; Burgueño, J.; Merlos, M.; Baeyens, J. M.; Giraldo, J.; López-García, J. A.; Maldonado, R.; Plata-Salamán, C. R.; Vela, J. M. Pharmacological properties of S1RA, a new sigma-1 receptor antagonist that inhibits neuropathic pain and activity-induced spinal sensitization. *Br. J. Pharmacol.* **2012**, *166*, 2289−2306.
(41) Díáz, J. L.; Christmann, U.; Fernández, A.; Torrens, A.; Port, A.; Pascual, R.; Álvarez, I.; Burgueño, J.; Monroy, X.; Montero, A.; Balada, A.; Vela, J. M.; Almansa, C. Synthesis and structure-activity relationship study of a new series of selective σ_1 receptor ligands for the treatment of pain: 4-aminotriazoles. *J. Med. Chem.* **2015**, *58*, 2441−2451.
(42) Lan, Y.; Chen, Y.; Xu, X.; Qiu, Y.; Liu, S.; Liu, X.; Liu, B. F.; Zhang, G. Synthesis and biological evaluation of a novel sigma-1 receptor antagonist based on 3,4-dihydro-2(*1H*)-quinolinone scaffold as a potential analgesic. *Eur. J. Med. Chem.* **2014**, *79*, 216−230.
(43) Lan, Y.; Chen, Y.; Cao, X.; Zhang, J.; Wang, J.; Xu, X.; Qiu, Y.; Zhang, T.; Liu, X.; Liu, B. F.; Zhang, G. Synthesis and biological evaluation of novel sigma-1 receptor antagonists based on pyrimidine scaffold as agents for treating neuropathic pain. *J. Med. Chem.* **2014**, *57*, 10404−10423.
(44) Glennon, R. A.; Ablordeppey, S. Y.; Ismaiel, A. M.; el-Ashmawy, M. B.; Fischer, J. B.; Howie, K. B. Structural features important for σ_1 receptor binding. *J. Med. Chem.* **1994**, *37*, 1214−1219.
(45) Glennon, R. A. Pharmacophore identification for sigma-1 (σ_1) receptor binding: application of the "deconstruction-reconstruction-elaboration" approach. *Mini-Rev. Med. Chem.* **2005**, *5*, 927−940.
(46) Asif, M. Some recent approaches of biologically active substituted pyridazine and phthalazine drugs. *Curr. Med. Chem.* **2012**, *19*, 2984−2991.
(47) Asif, M. A mini review on biological activities of pyridazinone derivatives as antiulcer, antisecretory, antihistamine and particularly against histamine H_3R. *Mini-Rev. Med. Chem.* **2015**, *14*, 1093−1103.
(48) (a) Kunitomo, J.; Yoshikawa, M.; Fushimi, M.; Kawada, A.; Quinn, J. F.; Oki, H.; Kokubo, H.; Kondo, M.; Nakashima, K.; Kamiguchi, N.; Suzuki, K.; Kimura, H.; Taniguchi, T. Discovery of 1-[2-fluoro-4-(1H-pyrazol-1-yl)phenyl]-5-methoxy-3-(1-phenyl-1H-pyrazol-5-yl)pyri dazin-4(1H)-one (TAK-063), a highly potent, selective, and orally active phosphodiesterase 10A (PDE10A) inhibitor. *J. Med. Chem.* **2014**, *57*, 9627−9643. (b) Hu, E.; Chen, N.; Bourbeau, M. P.; Harrington, P. E.; Biswas, K.; Kunz, R. K.; Andrews, K. L.; Chmait, S.; Zhao, X.; Davis, C.; Ma, J.; Shi, J.; Lester-Zeiner, D.; Danao, J.; Able, J.; Cueva, M.; Talreja, S.; Kornecook, T.; Chen, H.; Porter, A.; Hungate, R.; Treanor, J.; Allen, J. R. Discovery of clinical candidate 1-(4-(3-(4-(1H-benzo[d]imidazole-2-carbonyl)phenoxy)pyrazin-2-yl)piperidin-1-yl)e thanone (AMG 579), a potent, selective, and efficacious inhibitor of phosphodiesterase 10A (PDE10A). *J. Med. Chem.* **2014**, *57*, 6632−6641.
(49) Lima, L. M.; Barreiro, E. J. Bioisosterism: a useful strategy for molecular modification and drug design. *Curr. Med. Chem.* **2005**, *12*, 23−49.
(50) Viegas-Junior, C.; Danuello, A.; da Silva Bolzani, V.; Barreiro, E. J.; Fraga, C. A. Molecular hybridization: a useful tool in the design of new drug prototypes. *Curr. Med. Chem.* **2007**, *14*, 1829−1852.
(51) (a) Johnston, K. A.; Allcock, R. W.; Jiang, Z.; Collier, I. D.; Blakli, H.; Rosair, G. M.; Bailey, P. D.; Morgan, K. M.; Kohno, Y.; Adams, D. R. Concise routes to pyrazolo[1,5-a]pyridin-3-yl pyridazin-3-ones. *Org. Biomol. Chem.* **2008**, *6*, 175−186. (b) Druey, J.; Hucni, A.; Ringier, B. H.; Staehelin, A. Halogen pyridazines. US 2963477 A, 1960.
(52) Kowalski, P.; Kowalska, T.; Mokrosz, M. J.; Bojarski, A. J.; Charakchieva-Minol, S. Biologically active 1-arylpiperazines. synthesis of new N-(4-aryl-1-piperazinyl)alkyl derivatives of quinazolidin-4(*3H*)-one, 2,3-dihydrophthalazine-1,4-dione and 1,2-dihydropyridazine-3,6-dione as potential serotonin receptor ligands. *Molecules* **2001**, *6*, 784−795.
(53) Bojarski, A. J.; Kowalski, P.; Kowalska, T.; Duszynska, B.; Charakchieva-Minol, S.; Tatarczynska, E.; Klodzinska, A.; Chojnacka-Wojcik, E. Synthesis and pharmacological evaluation of new arylpiperazines. 3-[4-[4-(3-chlorophenyl)-1-piperazinyl]butyl]-quinazolidin-4-one - a dual serotonin 5-HT_{1A}/5-HT_{2A} receptor ligand with an anxiolytic-like activity. *Bioorg. Med. Chem.* **2002**, *10*, 3817−3827.
(54) DeHaven-Hudkins, D. L.; Fleissner, L. C.; Ford-Rice, F. Y. Characterization of the binding of [^{3}H](+)-pentazocine to sigma recognition sites in guinea pig brain. *Eur. J. Pharmacol., Mol. Pharmacol. Sect.* **1992**, *227*, 371−378.
(55) (a) Balasuriya, D.; D'Sa, L.; Talker, R.; Dupuis, E.; Maurin, F.; Martin, P.; Borgese, F.; Soriani, O.; Edwardson, J. M. A direct interaction between the sigma-1 receptor and the hERG voltage-gated K+ channel revealed by atomic force microscopy and homogeneous time-resolved fluorescence (HTRF(R)). *J. Biol. Chem.* **2014**, *289*, 32353−32363. (b) Diaz, G. J.; Daniell, K.; Leitza, S. T.; Martin, R. L.; Su, Z.; McDermott, J. S.; Cox, B. F.; Gintant, G. A. The [^{3}H]dofetilide binding assay is a predictive screening tool for hERG blockade and proarrhythmia: Comparison of intact cell and membrane preparations

DOI: 10.1021/acs.jmedchem.5b01416
J. Med. Chem. XXXX, XXX, XXX−XXX

and effects of altering $[K+]_o$. *J. Pharmacol. Toxicol. Methods* **2004**, *50*, 187−199. (c) Recanatini, M.; Poluzzi, E.; Masetti, M.; Cavalli, A.; De Ponti, F. QT prolongation through hERG K (+) channel blockade: current knowledge and strategies for the early prediction during drug development. *Med. Res. Rev.* **2005**, *25*, 133−166.

(56) (a) Hayashi, T.; Su, T. P. Regulating ankyrin dynamics: Roles of sigma-1 receptors. *Proc. Natl. Acad. Sci. U. S. A.* **2001**, *98*, 491−496. (b) Tsai, S. Y.; Pokrass, M. J.; Klauer, N. R.; Nohara, H.; Su, T. P. Sigma-1 receptor regulates Tau phosphorylation and axon extension by shaping p35 turnover via myristic acid. *Proc. Natl. Acad. Sci. U. S. A.* **2015**, *112*, 6742−6747.

(57) Wu, Z.; Bowen, W. D. Role of sigma-1 receptor C-terminal segment in inositol 1,4,5-trisphosphate receptor activation: constitutive enhancement of calcium signaling in MCF-7 tumor cells. *J. Biol. Chem.* **2008**, *283*, 28198−28215.

(58) Hayashi, T.; Su, T. P. Sigma-1 receptor chaperones at the ER-mitochondrion interface regulate Ca^{2+} signaling and cell survival. *Cell* **2007**, *131*, 596−610.

(59) (a) Cobos, E. J.; Baeyens, J. M.; Del Pozo, E. Phenytoin differentially modulates the affinity of agonist and antagonist ligands for sigma-1 receptors of guinea pig brain. *Synapse* **2005**, *55*, 192−195. (b) Maricel, G. S.; Víctor, F. D.; Enrique, P. S.; Pilar, P.; Daniel, Z.; Vela, J. M.; Javier, B.; Francisco, C. Predicting the antinociceptive efficacy of σ1 receptor ligands by a novel receptor fluorescence resonance energy transfer (FRET) based biosensor. *J. Med. Chem.* **2014**, *57*, 238−242.

(60) Rosland, J. H.; Tjolsen, A.; Maehle, B.; Hole, K. The formalin test in mice: effect of formalin concentration. *Pain* **1990**, *42*, 235−242.

(61) Cendán, C. M.; Pujalte, J. M.; Portillo-Salido, E.; Baeyens, J. M. Antinociceptive effects of haloperidol and its metabolites in the formalin test in mice. *Psychopharmacology* **2005**, *182*, 485−493.

(62) (a) Bennett, G. J.; Xie, Y. K. A peripheral mononeuropathy in rat that produces disorders of pain sensation like those seen in man. *Pain* **1988**, *33*, 87−107. (b) Chaplan, S. R.; Bach, F. W.; Pogrel, J. W.; Chung, J. M.; Yaksh, T. L. Quantitative assessment of tactile allodynia in the rat paw. *J. Neurosci. Methods* **1994**, *53*, 55−63.

(63) Caspani, O.; Reitz, M. C.; Ceci, A.; Kremer, A.; Treede, R. D. Tramadol reduced anxiety-related and depression-associated behaviors presumably induced by pain in the chronic constriction injury model of neuropathic pain in rats. *Pharmacol., Biochem. Behav.* **2014**, *124*, 290−296.

(64) Chou, J. C.; Czobor, P.; Charles, O.; Tuma, I.; Winsberg, B.; Allen, M. H.; Trujillo, M.; Volavka, J. Acute mania: haloperidol dose and augmentation with lithium or lorazepam. *J. Clin. Psychopharmacol.* **1999**, *19*, 500−505.

(65) Kiang, M.; Daskalakis, Z. J.; Christensen, B. K.; Remington, G.; Kapur, S. Actigraphic measurement of the effects of single-dose haloperidol and olanzapine on spontaneous motor activity in normal subjects. *J. Psychiatry Neurosci.* **2003**, *28*, 293−299.

(66) Sheldrick, G. M. A short history of SHELX. *Acta Crystallogr., Sect. A: Found. Crystallogr.* **2008**, *64*, 112−122 (SHELXTL versions 6.12 and 6.14).

(67) Bradford, M. M. A rapid and sensitive method for the quantitation of microgram quantities of protein utilizing the principle of protein-dye binding. *Anal. Biochem.* **1976**, *72*, 248−254.

(68) Diáz, J. L.; Christmann, U.; Fernández, A.; Luengo, M.; Bordas, M.; Enrech, R.; Carro, M.; Pascual, R.; Burgueño, J.; Merlos, M.; Benet-Buchholz, J.; Cerón-Bertran, J.; Ramírez, J.; Reinoso, R. F.; Fernández de Henestrosa, A. R.; Vela, J. M.; Almansa, C. Synthesis and biological evaluation of a new series of hexahydro-2H-pyrano[3,2-c]quinolines as novel selective σ_1 receptor ligands. *J. Med. Chem.* **2013**, *56*, 3656−3665.

DOI: 10.1021/acs.jmedchem.5b01416
J. Med. Chem. XXXX, XXX, XXX−XXX